DM

Fighting Dengue and Zika using novel Glycodendrimer-encapsulated metal nanoparticles as viral entry inhibitors
MASTER DISSERTATION

Natacha Manuel Pereira Rodrigues Antunes
MASTER IN NANOCHEMISTRY AND NANOMATERIALS

UNIVERSIDADE da MADEIRA
A Nossa Universidade
www.uma.pt

December | 2020

Fighting Dengue and Zika

using novel Glycodendrimer-encapsulated metal nanoparticles as viral entry inhibitors
MASTER DISSERTATION

Natacha Manuel Pereira Rodrigues Antunes
MASTER IN NANOCHEMISTRY AND NANOMATERIALS

ORIENTATION
Carla Sophia Brazão Andrade Sousa Alves

CO-ORIENTATION
João Manuel Cunha Rodrigues

Fighting Dengue and Zika using novel glycodendrimer-encapsulated metal nanoparticles as viral entry inhibitors

Thesis presented to University of Madeira for obtention of Master Degree in Nanochemistry and Nanomaterials

By Natacha Manuel Pereira Rodrigues Antunes

With supervision of Carla S. Alves and

co-supervision of Professor João Manuel Cunha Rodrigues

Declaration

I hereby declare that this thesis is the result of my own work, is original and was written by me.
I also declare that its reproduction and publication by Madeira University will not break any
third-party rights and that I have not previously (in whole or in part) submitted it elsewhere for
obtaining any qualification or degree.
Furthermore, I certify that all sources of information used in the thesis were properly cited.

Funchal, 15th December of 2020

Natascha

ACKNOWLEDGMENTS

First and foremost, I would like to thank my amazingly caring supervisor, PhD Carla Alves who supported me through my journey and never stopped trusting and believing in me. Without her supervision, guidance, companionship and willingness to help either in lab context or with the long discussions we had about arising obstacles along the way or near the end of it, this work would not have come to fruition.

I would also like to express my gratitude to my co-supervisor, Professor João Rodrigues for the guidance, patience, and valuable input in our discussions about several topics. The advice he gave me not only throughout the course of this project, but also during the Master Degree as a whole has helped shape my personality in a myriad of ways, be it either professionally or personally.

Additionally, I would like to kindly thank the precious help given by my colleagues from the Molecular Materials Research Group (MMRG) lab, MsC Ana Olival, Mara Gonçalves, Nilsa Oliveira and Duarte Fernandes. All of them heavily contributed in the simplest, yet crucial ways by either helping me with scientific input in discussions about random hypotheses that would come up or by accompanying me in some parts of the laboratory work, such as characterization of my samples via the NMR analyses.

Many thanks to the laboratory technicians from the Chemistry Department, Paula Andrade and Paula Vieira for all the kindness and readiness in providing some lab materials and reagents that I needed for this project.

Laboatório de Análises Químicas do Instituto Superior Técnico (LAIST) de Lisboa was also very much appreciated.

My sincere gratitude to my friends, who have unconditionally been by my side. To my all-time friend and colleague Gonçalo Martins for all the support, effort and patience put into me. Not only did he help me from a scientific standpoint but also as a friend, by encouraging me to go further and face my fears. Furthermore, to Emanuel Gouveia, Joanna Pataca, Anísia Martins and Diogo Mendonça for always being there for me and lifting my spirits.

Last, but definitely not least, to my beloved family who are my safe haven. My mom Teresa Rodrigues who brought me into this world and moulded who I am today through the values she passed on to me ever since I was born, up until now and for being my role model. To my aunt Helena Rodrigues who, similarly to my mom, has also shaped me into who I am and diligently continues doing so. To my grandparents Maria Zita and Leonel Rodrigues, my aunts Vanda Rodrigues, Paula Gomes and Maria da Luz Noronha, as well as my uncle Luís Gomes who in a way or another contributed to my growth as a person and inspired me to keep going even when times were rough.

Words are not enough to express my gratitude towards everyone who contributed in my progression towards the final goal.

LIST OF PUBLICATIONS

Part of the results and findings of this work were presented in the following:

Oral communications:

- Antunes, N., Tomás, H., Castanho, M. A. R. B., Alves, C. S., Rodrigues, J.; Synthesis and stability of PAMAM and PEI-entrapped copper nanoparticles, February 3-4, Funchal, Portugal, 2017.

Poster communications:

- Alves, C. S., Antunes, N., Tomás, H., Castanho, M. A. R. B., Rodrigues, J.; Synthesis of Novel Surface Modified Dendrimers for Dengue and Zika Viral Entry Inhibition (IDS11), July 14-18, Funchal, Portugal, 2019.

RESUMO

Os graves sintomas causados por doenças infeciosas, como, as febres dengue e zika são considerados nos dias de hoje um problema global que deve ser devidamente avaliado e combatido.[1] Com o intuito de fazer face às complicações associadas a estas duas enfermidades reemergentes, esforços têm sido direcionados para a descoberta de novos agentes antivirais, capazes de impedir a transmissão dos agentes causadores dessas patologias. Uma das estratégias assenta em saturar o recetor que promove a entrada destas partículas virais – DC-SIGN – nas células hospedeiras.[2] O recetor do tipo lectina, o DC-SIGN, é ativado por carbohidratos, monoméricos ou não. As semelhanças com os sacarídeos e as respetivas propriedades, despertaram recentemente o interesse da comunidade científica para a descoberta de glicomiméticos, moléculas especificamente capazes de serem utilizadas como substitutas das originais. Entretanto, estudos mostraram que o ácido chiquímico (SA) é uma boa opção para substituir os sacarídeos envolvidos na ativação do DC-SIGN. O presente trabalho teve como objetivo a criação de um sistema eficaz na captação da inigualável multivalência dos dendrímeros, no caso presente, os poly(amidoamina) (PAMAM) e das propriedades do SA, enquanto glicomimético. Nesse sentido, duas gerações de PAMAM (G4 e G5) foram funcionalizadas com SA por via do acoplamento mediado por carbodiimida EDC/NHS, obtendo-se assim PAMAM funcionalizados com SA (SAGx). Adicionalmente, e uma vez que as nanopartículas metálicas são conhecidas pela sua atividade antiviral, após purificação daqueles dendrímeros, procedeu-se à redução de cobre, mediada pelo ácido ascórbico. A caracterização dos complexos foi efetuada através de espectroscopias de Ultravioleta-Visível (UV-Vis), fluorescência, e de Infravermelho por Reflexão Total Atenuada (ATR-FTIR), ainda *Dynamic Light Scattering* (DLS), Ressonância Magnética Nuclear de protão (^{1}H RMN), Microscopia Electrónica de Varrimento (SEM) e *Inductively coupled plasma optical emission spectroscopy* (ICP-OES). Por fim, foi testada a citotoxicidade dos compostos SAGx, num intervalo de concentrações, em células HEK 293T. Das concentrações utilizadas verificou-se que a viabilidade celular sofreu um decréscimo acentuado a partir dos 400 µM para o SAG4. Em contrapartida, não se verificou grande variação para o SAG5, mesmo utilizando a concentração de trabalho máxima, 500 µM.

Palavras-chave: Glicomiméticos, nanopartículas de cobre, DC-SIGN, ácido chiquímico, células HEK 293T.

ABSTRACT

Due to their mild-to-severe symptoms, dengue and zika fevers are considered a global problem that must be assessed and acted upon.[1] In order to overcome the problems associated with these two re-emergent infectious diseases, research has focused on developing antiviral therapeutic agents that inhibit disease transmission. One strategy lies in blocking the dendritic cell-specific ICAM3-grabbing nonintegrin (DC-SIGN) receptor that the dengue virus (DENV) and the zika virus (ZIKV) both use to promote their entry into host cells. Being a lectin-type receptor, DC-SIGN is triggered by carbohydrate moieties. Recently, because of similarities with saccharides, great efforts have been placed into discovering new glycomimetics that can be used as sugar alternatives. Previous studies have shown shikimic acid (SA) to be a good glycomimetic contender in targeting the DC-SIGN receptor.[2] This work aimed to develop a system that effectively targets DC-SIGN by taking advantage of the unique multivalency and conjugation versatility of the poly(amidoamine) (PAMAM) dendrimers and combine it with the properties of SA. Amine-terminated generation four ($G4.NH_2$) and generation five ($G5.NH_2$) PAMAM dendrimers served as scaffolds to conjugate SA via the EDC/NHS coupling method to obtain the corresponding SA-functionalized dendrimers (i.e., SAG4 and SAG5). The formed conjugates were then used to as templates to prepare copper dendrimer entrapped nanoparticles (Cu DENPs). All of the complexes underwent characterisation via Ultraviolet-Visible (UV-Vis) spectroscopy, fluorescence spectroscopy, Attenuated Total Reflectance-Fourier Transform Infrared spectroscopy (ATR-FTIR), Dynamic Light Scattering (DLS), proton Nuclear Magnetic Resonance (^{1}H NMR), Scanning Electron Microscopy (SEM) and ICP. *In vitro* analysis of the cytotoxic effects of the SAG4 and SAG5 compounds obtained from the first reaction step was assessed in HEK 293T cells. Having tested a wide range of different glycomimetic concentrations, it was found that cell viability decreased significantly when using a concentration of 400 µM for SAG4. For SAG5, on the other hand, no significant impact on cell viability was observed, even when using a 500 µM concentration.

Keywords: Glycodendrimers, Cu DENPs, DC-SIGN, Shikimic acid, HEK 293T cells.

Table of Contents

List of Tables

List of Figures

List of Acronyms

ADE – Antibody-dependent enhancement

APCs – Antigen-presenting cells

Asn - Asparagine

BG – Birbeck granules

CRD – Carbohydrate recognition domain

CTL – C-type lectin

CuSAG4 – Shikimic acid-functionalised generation 4 PAMAM stabilized copper nanoparticles

CuSAG5 – Shikimic acid-functionalised generation 5 PAMAM stabilized copper nanoparticles

DBV – *Dakar bat virus*

DCs – Dendritic cells

DC-SIGN – Dendritic cell-specific ICAM3-grabbing nonintegrin

DENV – *Dengue virus*

DKG – 2,3-diketogluconic acid

D$_2$O – Deuterated water

EDC – 1-Ethyl-3-(3-dimethylaminopropyl)carbodiimide

FDA – Food and Drug Administration

FTIR – Fourier Transform Infrared Spectroscopy

G4 – Generation 4

G5 – Generation 5

GalNAc – N-acethylgalactosamine

HCV – Hepatitis C virus

HIV - Human Immunodeficiency virus

IR – Infrared

ICP-OES – Inductively coupled plasma optical emission spectroscopy

ICP-AES – Inductively coupled plasma atomic emission spectroscopy

JEV – *Japanese encephalitis virus*

LCs – Langerhans cells

L-SIGN – liver/lymph node-specific ICAM3-grabbing integrin

m – Multiplet

MWCO - Molecular weight cut-off

MHC - Major histocompatibility complex

NaOH – Sodium hydroxide

n.d. – Not defined

NHS – N-Hydroxysuccinimide

NK – Neutral killer cells

NMR – Nuclear Magnetic Resonance

NP – Nanoparticle

NS – Non-structural

PAMAM – Polyamidoamine

PAMP - Pathogen-associated molecular patterns

PDI – polydispersity index

ppm – Parts per million

q – Quartet

RdRP – RNA-dependent RNA polymerase

RER – Rough endoplasmic reticulum

RNA – Ribonucleic acid

s – Singlet

SAG4 – Shikimic acid-functionalised generation 4 PAMAM

SAG5 – Shikimic acid-functionalised generation 5 PAMAM

Ser – Serine

ssRNA – single strand ribonucleic acid

SLEV – *Saint Louis encephalitis virus*

TAM - Tyro3, Axl, and Mertk

TCR – T cell receptor

Thr – Threonine

TIM – T cell immunoglobulin

TM – transmembrane

t – Triplet

WNV – *West Nile virus*

ZIKV – *Zika virus*

^{1}H-NMR – Proton Nuclear Magnetic Resonance

CHAPTER 1 – INTRODUCTION

1.1. Dengue and zika in context

The first reported evidence of dengue occurred back in 1779 in Java[3–6], while zika on the other hand, was first reported in 1947, in Uganda.[7] Since these, other chronologically separated events have happened. In the case of dengue, there were reports of massive outbreaks in 2010 (Croatia), 2012 (Madeira Island) and 2016 (Brazil, Philippines and Malaysia), and a sharp increase in the number of cases happening worldwide has since been noticed.[8] On the other hand, zika outbreaks were reported in 2007 (Pacific Island of Yap), 2013/2014 (French Polynesia, Easter Island, Cook Island, and New Caledonia) and 2018 (Brazil, Mexico, and Bolivia).[9,10] Because of this, these infectious diseases have been targeted by not only governmental entities of risk areas, but also by the World Health Organisation (WHO).

Overall, the *Dengue virus* (DENV) induces flu-like symptoms such as high fever (usually higher than 40ºC), fatigue and myalgia (muscle pain), along with headaches, retro-orbital pain, skin rash, nausea, vomiting, arthralgia (joint pain) and occasionally some mild bleeding (mainly in the gums and nosebleeds).[11] Depending on the age and immune system of the individual, the medical state can evolve into something more worrisome, such as haemorrhagic fever, liver enlargement and damage to the circulatory system. The factor that contributes to the severity of the symptomatology at a first stage, however, is the serotype of the virus that has been contracted (DENV-1, DENV-2, DENV-3 or DENV-4).[12]

Thus far, there is no specific treatment for dengue, other than what you would do for the common flu: lots of rest, be sure to stay hydrated and wait for the symptoms to subside after approximately 2 to 7 days. In case there is a need to manage fever, acetaminophen should be used instead of aspirin or other nonsteroidal anti-inflammatory drugs due to the increased risk of Reye's syndrome.[13] Once the infection is cured, the individual gains lifelong immunity to the specific serotype he/she was infected with. However, in the case of secondary infection by any of the other serotypes, the disease can develop into severe dengue, which is when the symptoms are harsher than they would be otherwise and it may ultimately lead to death.[14]

In addition to the flu-like symptoms that DENV exhibits, patients infected with the *Zika virus* (ZIKV) also manifest non-purulent conjunctivitis, swollen hands and ankles, subcutaneous bleeding and hematospermia.[12,15] And, just like dengue, the morbidity rate associated with zika is rather low.[12,16,17] Moreover, there is a high probability that zika is linked to the incidence of

Guillian-Barré syndrome. It has also been shown that the symptoms associated with zika are aggravated by pre-existing conditions such as meningoencephalitis and acute myelitis.[18,19]

Strong evidence shows that in addition to the conventional mode of transmission (i.e., mosquito bite), which is the only means used by DENV, ZIKV can also be transmitted between humans either via sexual intercourse or from mother to foetus and even through blood transfusions.[7,15,20,21] This opens the door for more complications in addition to those that are usually associated with this infectious disease, especially in the case of vertical transmission. Due to the fact that ZIKV is able to permeate the placenta, it can cause a series of foetal abnormalities including microcephaly, intellectual disability, ischemic brain damage, cerebral palsy, cardiac and eye anomalies, and sensorineural hearing loss.[16]

Much like dengue, zika has no specific treatment other than what is recommended for dengue. Moreover, no pre-emptive measures exist for it so far. Since the spread of ZIKV can be done via horizontal transmission, the use of protection during sexual intercourse is sufficient.[7] However, if a pregnant woman is bitten by a mosquito, it can still lead to foetal malformations. In this case, the baby must receive specialised care after birth.[22]

Due to all the complications that stem from both these infectious diseases, it is of utmost importance to find ways to deter their spread. In order to do so, it is important to understand the route of viral infection – the vector. The primary carriers of both DENV and ZIKV belong to the *Aedes aegypti* and *Aedes albopictus* species, each originating from Africa and Southeast Asia, respectively. And, since they are carried by mosquitos, both DENV and ZIKV fall under the category of arboviruses, with the word originating from *ar(thropod)-bo(rne)* and *virus*. Both species breed in habitats close to humans, usually ones that are warm and humid, and they have also occasionally been found in forests.[23] Although initially limited to those areas, their small size and incredible mobility, combined with the transportation of goods and people abroad, has led to their further spread, and they are now also located in Europe and the American Continent (mainly Brazil). Besides dengue and zika, these vectors are also associated with the spread of chikungunya and yellow fever.[24,25]

It is known that although *Ae. aegypti* and *Ae. albopictus* can be active during the daytime, the females tend to be the most active during dusk and dawn while they are blood-feeding. These species often fly low and lay their eggs in still waters.[25,26] Regardless of gender, both mosquitos

feed off of plant nectar. However, right before oviposition, the female gravitates towards blood in an attempt to obtain protein that it can use to feed its progeny.

The life cycle of the *Aedes* genus consists of four major stages: egg, larva, pupa, and lastly, the adult mosquito (see Fig. 1). Each female mosquito lays around 100 – 200 eggs per batch and can do so up to five times throughout its entire lifetime. After being laid in a body of water, under adequate temperature and humidity conditions usually facilitated by tropical and subtropical climates, the egg takes about 4 to 5 days to hatch. Once this happens, the now larva spends most of its time on the surface of the water, and occasionally dives to find food (e.g., algae and other microscopic organisms). The larva then transitions into a pupa over a period of 2 days and finally reaches adult form. Once it reaches its final form, it can at last take its first blood meal.[24]
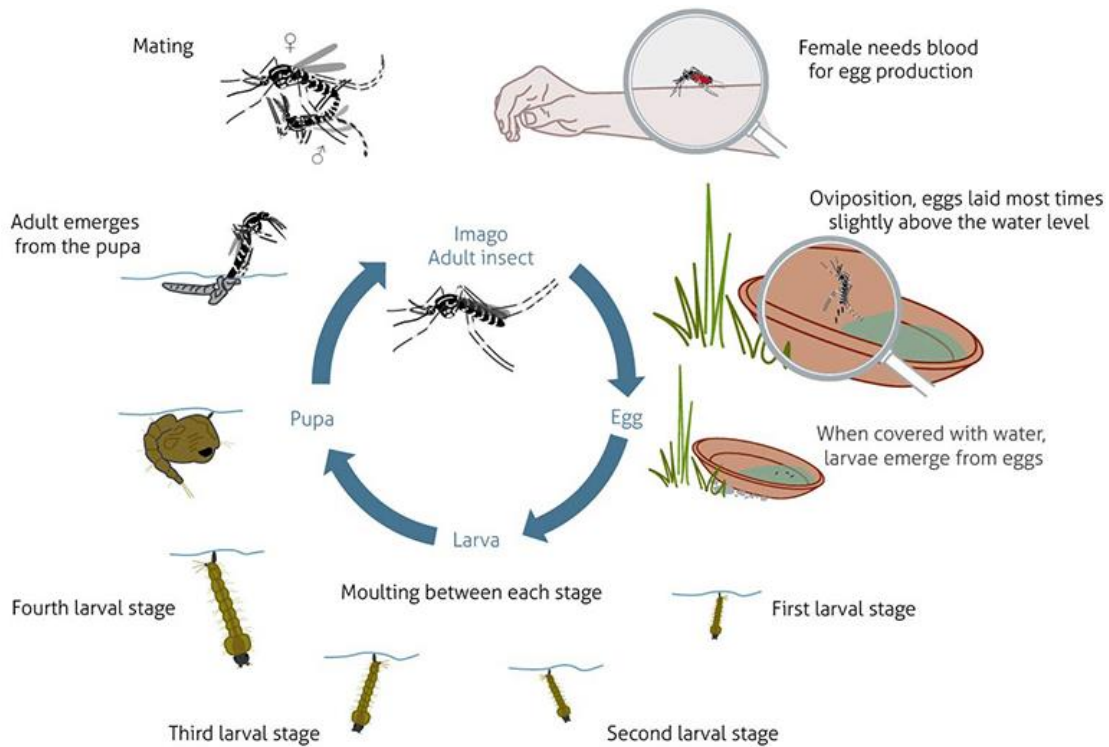
Figure 1 – The life cycle of the *Ae. aegypti* and *Ae. albopictus* species.[27]

The existing control measures based on the life cycle of the *Aedes* vectors can be divided into five categories: 1) chemical intervention (i.e., implementation of insecticides and larvicides)[28], 2) habitat management (i.e., controlling the availability of breeding sites)[29], 3) non-chemical intervention (i.e., use of larvivorous fish, oil coatings in waters and larvae traps)[30,31], 4) population replacement (i.e., insertion of sterile males in order to control the reproduction rate) and 5) genetic techniques (i.e., releasing mosquitos that have a gene that causes automatic death of offspring).[26,32]

The first, and arguably the most important step towards controlling the spread of dengue and zika relies on vector management. By having basic knowledge about the vector's life cycle or where the vector lays its eggs, anyone can have an active role in its management. This is why public education about the topic is important and why governmental entities should promote prevention campaigns, especially in the areas that are most affected by these epidemics.[33] Some measures that can be used by people in their households fall under the habitat management category and consist of draining all water deposits that are exposed (e.g., pot saucers, swimming pools, birdbaths, buckets, tyres, etc.), or alternatively, covering the containers with a mesh that is smaller than the mosquito itself. Furthermore, installing nets on windows is a good way to keep mosquitos away.[33,34] In addition, vaccination campaigns against the infectious diseases that these vectors spread is also a method of prevention that should be considered if you live in a risk area.[26] In the case of dengue, a vaccine targeted towards all DENV serotypes became available as of 2015. Dengvaxia®, developed by Sanofi Pasteur, is currently the only available pre-emptive measure for either infectious disease that has been approved and is commercially available.[35] As such, there is the need to direct efforts into expanding the variety of available options.

1.1.1. Virus morphology

From a biochemical standpoint, viruses are a combination of genetic material and proteins. These miniscule and simple particles, within a size range of 45 to 220 nm depending on the virus, are capable of causing a lot of damage to living organisms.[36] On a structural level, they are nothing more than genetic material (either DNA or RNA) with a protective capsule

around it. This capsule, also known as capsid, is a carefully engineered protein structure that fulfils the role of keeping the information to build new viral particles safe. In addition, some viruses can have an extra protective layer, the envelope, in which case they are denominated enveloped viruses. Those viruses that lack an envelope are deemed naked viruses.[37]

Taxonomically speaking, both DENV and ZIKV belong to the *Flaviviridae* family. More specifically, both viruses belong to the *Flavivirus* genus and as such are commonly referred to as flaviviruses. The *Yellow Fever Virus* (YFV) was the first virus of its kind to ever be reported, and as a consequence the name of the taxon it belongs to currently stems from the word *flavus*, which is Latin for yellow.[38] Over the years, other species have been added to this family including *West Nile Virus* (WNV), *Japanese Encephalitis Virus* (JEV), *Saint Louis Encephalitis Virus* (SLEV), *Dakar Bat Virus* (DBV), amongst others, to the point that the *Flavivirus* genus now amounts to a total of 53 species.[39–41]

Characteristically, flaviviruses have an envelope around the capsid and the genetic material consists of a single strand of positive sense RNA ((+)ssRNA) (see Fig. 2). The first layer of protection of flaviviruses, the envelope, consists of a lipid bilayer that has two types of protein: the envelope (E) protein (≈50 kDa) and the membrane (M) protein (≈8 kDa). Depending on the stage of maturation, there is a pre-membrane (prM) protein (≈26 kDa). The main role of the E protein is to assist in the attachment of the viral particle and promote its subsequent fusion with the membrane of the host cell.[42,43] On the other hand, the prM protein, which is only present in immature viral particles, is proteolytically cleaved into the M protein, the role of which is still unclear.[42,43] Finally, the last layer of protection of the flavivirus is the capsid, which is a conglomerate of several copies of basic capsid (C) proteins (≈11 kDa).[44] With the advent of molecular biology, conserved sequences of all these components have come to light. These sequences are intrinsically related to the function of each protein and are what make all viruses across the *Flavivirus* genus serologically related. This information is particularly useful in the diagnosis and prevention of the diseases caused by DENV and ZIKV, because their antigenic similarities make it easier to develop a system that can target multiple species at once.[42]
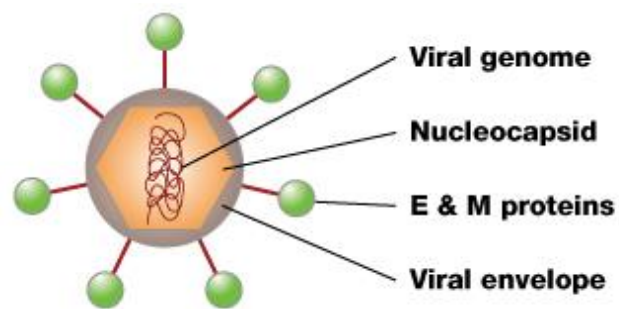
Figure 2 – General structure of flaviviruses.[45]

Although similar in their basic structure, differences exist in the key components of flaviviruses. One such difference resides in the structure of the E protein itself. In fact, it is known that DENV shares on average 55.6% of the amino acid sequence in its E protein with ZIKV.[46] In general, each monomer of this dimeric rod-like protein has four domains: a transmembrane (TM) domain and three ectodomains (see Fig. 3). In the case of the latter domains, the DI ectodomain plays a role in stabilising the orientation of the protein, DII partakes in virus-mediated membrane fusion and DIII binds the virus to the host receptor and works as an antigen thereby making it a good target in preventing viral attachment.[47–49] Upon translation, the E protein undergoes glycosylation. Two types of glycosylation may occur: (i) N-linked glycosylation, where a saccharide binds to the amide nitrogen in a specific asparagine (Asn) residue of the protein or (ii) O-linked glycosylation, where a saccharide is bound to an oxygen atom in the serine (Ser) or threonine (Thr) residues.[49] Although flaviviruses usually have two glycosylation sites, some viruses in this family only have one.[50] In the specific case of DENV, the E protein is known to undergo N-glycosylation in DI and DII on N67 and N153, respectively.[49] In the case of ZIKV, on the other hand, glycosylation is known to occur on residue N154.[51] The main role of this glycosylation process in the E protein of both DENV and ZIKV is to shape its conformation in order for it to perfectly fit the structure of the host receptor, hence facilitating the process of host cell infection. It is this intimate connection between the E protein and the process of viral infection that makes it a great target candidate in the battle against either DENV or ZIKV infection.
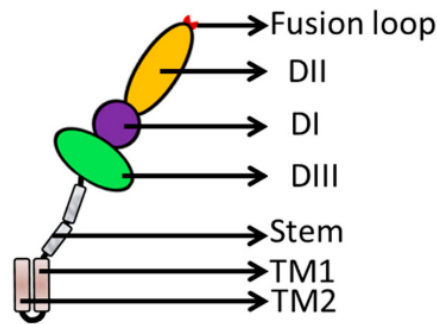
Figure 3 – Basic representation of a dimer of the E protein, which has three extracellular domains (DI, DII and DIII) that are bound to the transmembrane (TM) domains by the stem. Adapted from Ref[48]

All the information regarding the aforementioned protein components is present in the viral genome. The RNA strand of flaviviruses, which is approximately 11 kilobases in length, is divided into two main sections: the structural and the non-structural (NS) genes (see Fig. 4).[39,52] As depicted in the figure below, the structural genes code for proteins that give structure to the virus (i.e., protein C, prM and E).[40] On the other hand, the NS proteins are the ones involved in coordinating the replication and assembly of the new viral particles and they consist of several proteins addressed as NS1 through to NS5 according to the corresponding open reading frame (ORF) sequence.[42,53] In general terms, NS1 is a 46 kDa glycoprotein that can either exist in the host's cell, where it will be directly involved in the regulation of RNA replication, or in circulation though the host's body, where it will regulate complement activation, thus slowing down the natural immune response.[42,53] NS2A (22 kDa) and NS2B (15 kDa) are two integral membrane proteins, with NS2B known to cooperate with NS3 in proteolysis. NS3 is a 70 kDa protein that has two different components, one that acts as protease and another that has a ssRNA-stimulated triphosphatase-RNA-helicase. Similar to NS2A and NS2B, NS4A (15 kDa) and NS4B (29 kDa) are integral membrane proteins.[42] Finally, NS5 is a 100 kDa protein that works together with NS3 as part of the RNA-dependent RNA polymerase (RdRP), also known as RNA replicase.[42]
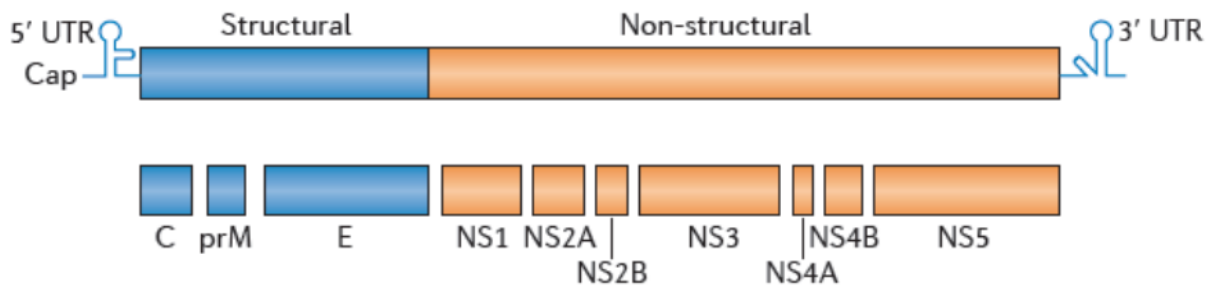
Figure 4 – Flaviviruses genome structure.[47]

1.1.2. Viral entry pathways

Upon being bitten by an infected mosquito, both DENV and ZIKV are released into the bloodstream and surrounding skin cells (e.g., keratinocytes and skin dendritic cells (DCs)) of the host. In each case, after the viral particles are captured by the DCs, they are then taken to secondary lymphoid organs where, if all goes smoothly, they will be eliminated by effector cells, in this case, T cells.[54,55] It is worth mentioning that flaviviruses target not only DCs, but also macrophages and B cells. However, because of the abundance of DCs in the human body and their predominant role in the immune system, combined with the fact that flaviviruses have been proven to preferably target these cells, numerous studies targeting dengue and zika revolve around receptors present on their surface.[54] As a part of the immune system, DCs, a type of professional antigen-presenting cells (APCs) that have their origin in bone marrow, fulfil the role of scanning the body for threats, reason for which they are seen as the sentinels of the immune system.[56] Besides the epidermis, DCs are scattered all over the body, in areas including in the lymph nodes, in the bloodstream and in the organs of the immune system.[57] Overall, the main role of these cells is to engulf bacteria, foreign particles and damaged cells, like macrophages would.

Although any type of DC can be targeted by flaviviruses, there are two types of DC subsets that are especially susceptible to infection, $CD14^+$ and Langerhans cells (LCs), both of which exist on the surface of the skin where the vector establishes the first contact with the host. Amongst a series of other surface receptors, $CD14^+$ expresses the dendritic cell-specific ICAM3-grabbing nonintegrin (DC-SIGN) and LCs express the langerin receptor, both of which are lectin homologues and are thus equally involved in the infection of flaviviruses.[39,58,59] In addition to these two receptors, a myriad of other surface molecules are proposed to play a role in the entry of flaviviruses into the host cell (see Fig. 5) through a process that is still not fully known. These include the liver/lymph node-specific ICAM3-grabbing integrin (L-SIGN) receptor, mannose receptors, phosphatidylserine receptors, T cell immunoglobulin and mucin domain (TIM) receptor, Tyro3, Axl, and Mertk (TAM) receptors, and the phospholipid receptor CD300a.[60,61] It is also known that facilitated infection by some flaviviruses such as DENV, ZIKV and YFV, a process also known as antibody-dependent enhancement (ADE), triggers the Fc receptor.[56,62,63] In the case of the DC-SIGN receptor, it is highly expressed in immature DCs and macrophage subpopulations, especially present in the dermis of the skin, mucosae, and in

lymph nodes. The L-SIGN receptor on the other hand is more abundant in endothelial cells specifically in liver sinusoids, lymph nodes, placenta, and in the gastrointestinal tract. [64]
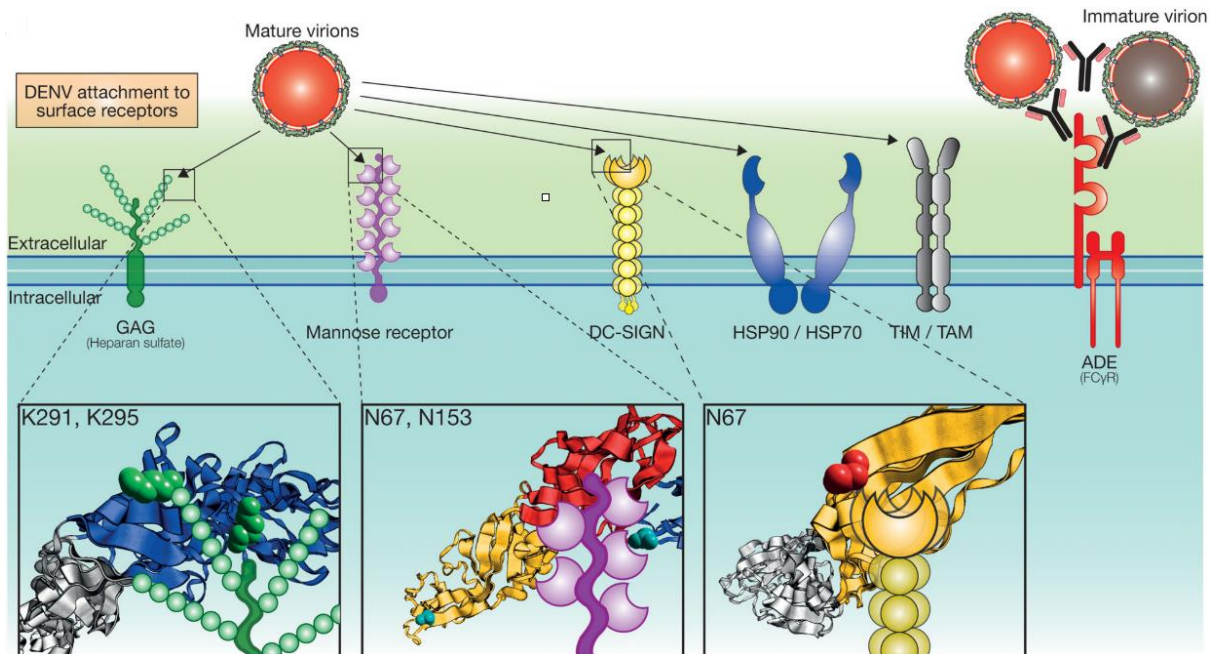
Figure 5 – Cell surface molecules that are potentially involved in the infection process of DENV and ZIKV. Adapted from Ref[1]

The life cycle of DENV is shown in Fig. 6, and due to the various similarities, this cycle may also be applied to ZIKV and arguably any other flavivirus.[60] The cycle involves (1) fully mature and some partially mature viral particles that (2) attach to surface receptors of the host cell and (3) enter the host cell through receptor-mediated endocytosis, also known as clathrin-dependent endocytosis, where the particles are entrapped within an endosomal vesicle that forms as a result of virus-receptor interaction.[60,65] In step (4) of the cycle, the acidic pH within the vesicle triggers conformational changes in the viral E protein, exposing the fusion peptide, leading to fusion between the viral and endosomal membranes, and thus allowing the nucleocapsid to be released into the cytoplasm.[60,65] Once the RNA leaves the capsid, it is presented to the rough endoplasmic reticulum (RER) for translation into a polyprotein that will be then cleaved by host and viral proteases into the three structural and seven non-structural proteins (5).[66,67] Following the synthesis of the viral replication complex, RNA translation ceases and viral antisense RNA transcription and amplification begins (6). The newly synthesised RNA is packaged with several copies of the C protein, forming the nucleocapsid (7).[68] After this, on the surface of the RER, viral assembly takes place when the nucleocapsid

buds into its lumen (8).[68] Finally, the immature viral particles go through the Golgi apparatus into the trans-Golgi network where they are subjected to a series of conformational changes that result in the exposure of cleavage sites and upon cleavage the viral particles are released.[69,70]
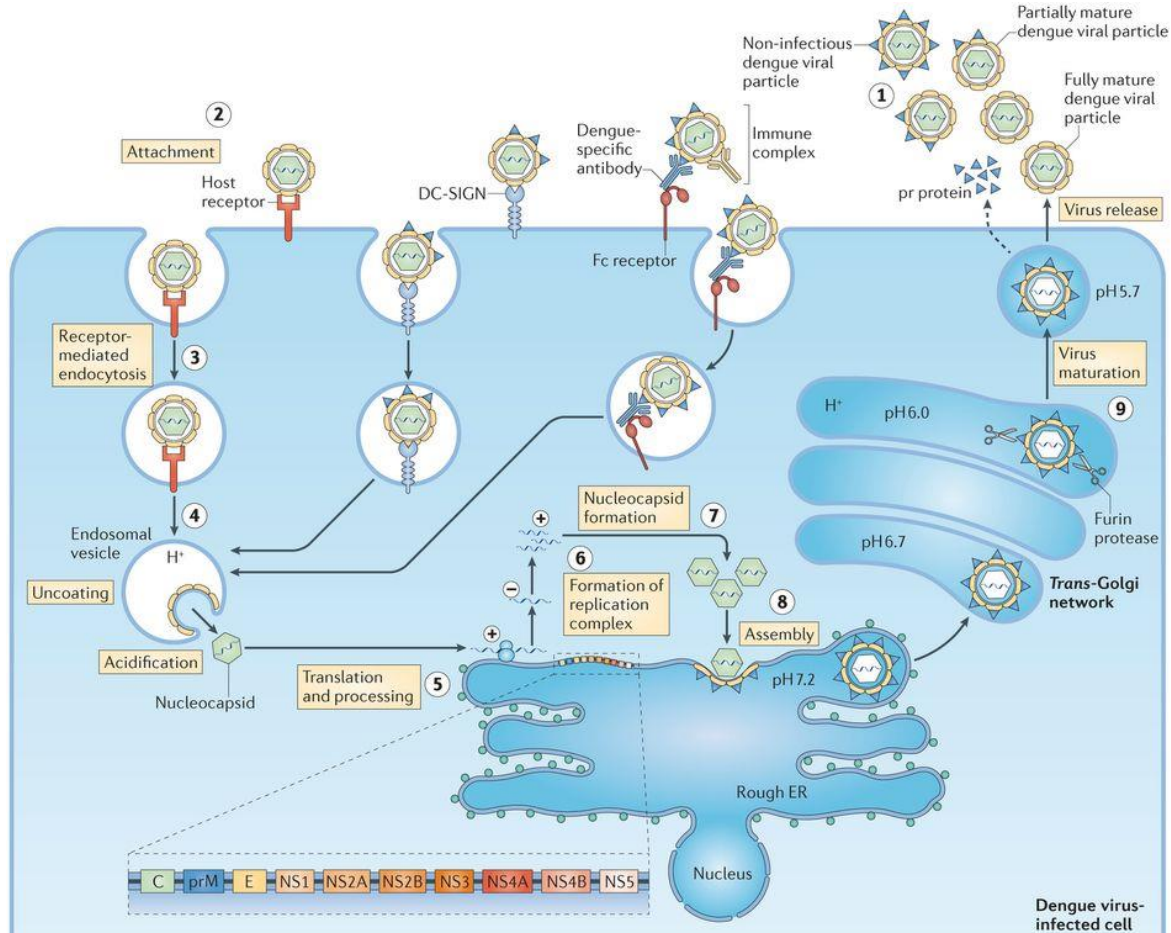
Figure 6 – Life cycle of DENV.[69]

There are several ways to intercept the action of flaviviruses, with all of them based on the virus life cycle, from the moment of first contact with the host cell until the virus finds itself inside the cell.[71,72] However, a viable strategy is to target viral entry into the host cell in order to minimise the repercussions of infection in the human body as much as possible. Potential antivirals can be designed bearing in mind the host cell receptor structure, which may be mimicked to produce similar molecules that will target the viral E protein and attach to it. On the other hand, the structure of the E protein of the virus may be reproduced to target the host cell receptors used by the virus for host cell infection.[65]

1.2. Receptors in the context of dengue and zika

Initially described by Peter Hermann Stillmark, in 1888, lectins, are present in a myriad of different organisms that range from animals to plants, and even bacteria.[73] Due to their high specificity binding to glycans, lectins are also known as carbohydrate-binding proteins or agglutinins and because of this, they are involved in several biological processes, such as the immune response, cell signalling, apoptosis, metastasis, and they have even been found to be involved in viral infection.[74,75] In addition, due to their biological roles, lectins have been used in a variety of different applications, such as insecticides, antimicrobials, antivirals, in antitumour drugs, and others.[76]

With the discovery of molecular biology, the intrinsic amino acid sequences of lectins has allowed for them to be grouped as either type I or type II lectins. The first group takes into consideration both the structural and evolutionary sequence similarities, while the second group consists of proteins without a particular evolutionary resemblance.[77] Due to the aim of this work, the focus will be on type I lectins, specifically, the C-type branch.[77]

C-type lectins (CTLs), otherwise known as calcium-dependent lectins, partake in important biological processes like cell adhesion, glycoprotein clearance, and innate immunity.[78] Unlike other families of lectins, which have preferential specificity towards a certain saccharide, CTLs present specificity for a wide selection of carbohydrates.[77] For the interaction with their antagonists to take place, they require the presence of Ca^{2+} as it directly secures the bond between the carbohydrate and the CTL binding site itself.[79] This binding pocket, exemplified by DC-SIGN in Fig. 7, is located in the carbohydrate recognition domain (CRD) of the CTL and is the portion of the protein that all the elements of this family have in common and that specifically binds to the terminal unit or typically referred to "core monosaccharide" of large carbohydrates. In practical terms, the Ca^{2+} is octacoordinated, meaning that it shares a total of 6 bonds with amino acid residues of the lectin and a total of 2 with the hydroxyl groups of the saccharide. Moreover, since the amino acid residues that bind to the carbohydrate are what determines the lectin specificity, this is what dictates which carbohydrate they have the highest affinity towards.[80]
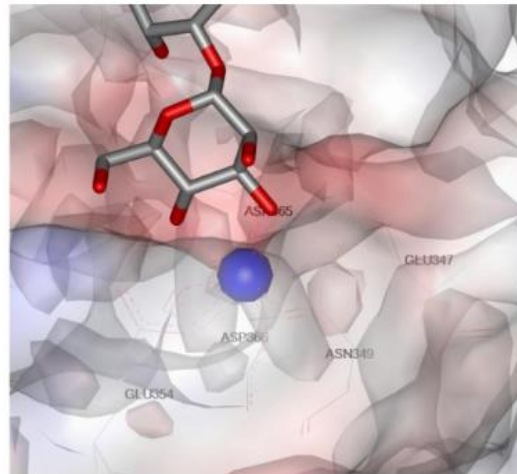
Figure 7 – Spatial arrangement of DC-SIGN in complex with Man$_4$ tetrasaccharide (PDB code: 1SL4)[81]. In the biding pocket, the 3- and 4-OH groups of the core monosaccharide (in sticks rendering and without hydrogens) coordinates to the Ca^{2+} atom (blue sphere) and establishes hydrogen bonds with amino acids around. Note that Ca^{2+} is octacoordinated and that, in order to provide a better visualisation, proteins are presented as transparent surfaces with amino acid residues (thin sticks). Adapted from Ref[80].

In the past, these lectins have been discovered to potentially facilitate viral infection into the cells of the immune system of the host where they are predominantly present.[82–84] As previously mentioned in section 1.1., this is due to the carbohydrate moieties present in the flavivirus E protein that are responsible for the interaction with the host cell receptors. In the specific case of dengue and zika, there are two carbohydrate binding proteins on the host cell surface that must be focused on: the DC-SIGN and Langerin. Both will be explored in more detail in the next section.

1.2.1. DC-SIGN receptor

First discovered in 2000, the DC-SIGN receptor, also called CD209, has been shown to be connected to a number of functions, such as DC differentiation from monocytes, antigen capture, T cell priming and mediating DC trans-endothelial migration.[80,85,86] Furthermore, this receptor has also been proven to facilitate infection of DCs by a number of pathogens, such as the influenza virus, the human immunodeficiency virus (HIV), and the hepatitis C virus (HCV), thereby leading to the trigger of an immune response.[64,87]

The DC-SIGN receptor, a type II transmembrane receptor, has an average 404 amino acids and a molecular weight of 44 kDa.[88] In an attempt to maximise the avidity of this lectin towards Pathogen-Associated Molecular Patterns (PAMPs) that exist in viral particles, the DC-SIGN receptor, illustrated in Fig. 8, is known to organise itself in tetramers on the cell membrane.[80] Each respective monomer is equivalent and has three domains – the intracellular, the intermembrane, and the extracellular one.[80] The first domain is responsible for transducing a signal upon carbohydrate binding, although the process for this is still not very well known. The second domain on the other hand keeps the CRD in place so as to promote binding. Finally, the extracellular domain is constituted by an elongated portion referred to as the neck and a globular structure that contains the CRD. The neck has seven and a half loops and is known to have an important role in the process of tetramerisation, while the CRD promotes pathogen recognition and subsequent internalisation.[89] When it comes to affinity, DC-SIGN shows a clear preference towards highly mannosylated glycans that are mainly present in enveloped viruses, as well as highly fucosylated oligosaccharides that are typical in parasites.[89] In all cases, the receptor-saccharide interaction is easily reversible as it is relatively weak in nature due to the fact that it is stabilised via hydrogen bonding with the hydroxyl groups in the ligand.[85,90] Moreover, the interaction of Ca^{2+} within binding site of the DC-SIGN receptor is established via four amino acids (Glu347, Asn349, Glu354 and Asn365), and as with any other C-type lectins, this is what dictates the carbohydrate specificity.[88]
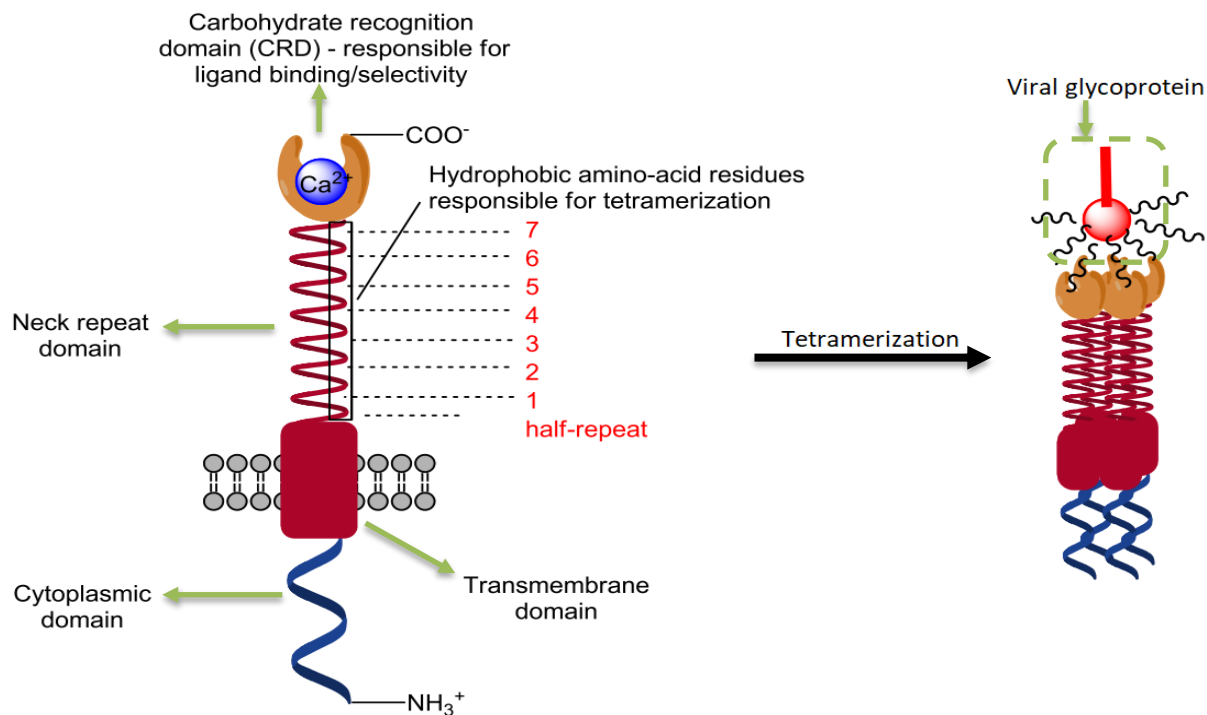
Figure 8 – The DC-SIGN monomer structure (left) and respective tetramerised form (right). Adapted from Ref[80]

1.2.2. Langerin receptor

First characterised in 2000, the langerin receptor, also known as CD207, is a homologue of DC-SIGN that exists exclusively in LCs.[91] As a type II C-type lectin, the langerin receptor fulfils the role of pathogen recognition and subsequent internalisation. This receptor has been linked to the infection of HIV-1 in the past, but unlike what happens in the case of DC-SIGN, the virus is captured by Birbeck granules (BG), exclusive organelles of LCs, which are in charge of degrading pathogens.[91,92] Although some information is available, the actual process that is triggered here upon ligand recognition is not yet fully understood.[59]

The langerin receptor is a 37.5 kDa protein that is 328 amino acids long.[91] It has an intracellular C-terminal domain, a transmembrane domain and an extracellular N-terminal domain where the CRD is located.[93] The latter comprises the neck region, which mediates the trimer organisation it preferentially adopts in the membrane.[94,95] In addition to mannose and fucose, langerin also recognizes N-acetylglucosamine, which grants LCs increased valency, resulting in a broader spectrum of pathogens that can be neutralised.[96]

1.3. Targeting the receptor

1.3.1. Glycochemistry

Glycochemistry entails a field of study dedicated to the investigation of carbohydrates and their interactions with biological systems.[97] Carbohydrates, also broadly referred to as glycans, comprehend any compounds bearing the stoichiometric formula $C_n(H_2O)_n$, specifically, aldoses and ketoses. This group of molecules includes all monosaccharides and derivatives, oligosaccharides, and polysaccharides of all kinds.[98] Studies throughout the years have shown saccharides to be associated with a myriad of biological functions, including receptor recognition, cell signalling and adhesion, inflammatory response, immunity, gene expression, fertilization, haematopoiesis and homeostasis.[78,97] As such, they have been implemented in numerous studies focussed on biomedical applications (e.g. drug delivery, tissue engineering, immunomodulation, etc.).[99] They have also been employed in the field of energy and materials science.[78,100]

The use of carbohydrates as drugs can be a delicate subject to handle. The main reason for this is because they are the main source of energy of the human body, which means that they are quickly metabolised once ingested. In addition to this, carbohydrates do not fulfil the requirements of classic drugs, as they exhibit poor pharmacokinetics, bioavailability, stability, and low affinity.[78] Furthermore, it has been previously determined that due to their nature, they are, for the most part, unable to passively bypass the enterocyte layer located in the small intestine, and therefore, are also prone to rapid excretion.[80] Due to these intrinsic liabilities, more research has been geared towards finding carbohydrate-based alternatives that overcome these problems, and this is how the branch of glycomimetics was born.

1.3.2. Glycomimetics

In the field of glycomimetics, an important factor to consider is the interaction between receptors and their respective counterparts, as is illustrated by the well-known Fisher's "lock-key" model.[97] It accurately, yet simply describes how the ligand, represented by the "key", interacts with the receptor, which is represented by the "lock". By understanding the dynamic between the receptor and its natural antagonists, it is possible to build ligands that fit the exact characteristics of the binding pocket of the target receptor.[97]

By definition, glycomimetics consists of designing molecules based on the bioactive conformation of the target native carbohydrate that have a similar structure to saccharides but do not necessarily possess the same nature.[97] In both the DENV and ZIKV particles, surface carbohydrates are widely dispersed throughout its extension as exemplified by Fig. 9.[66] These molecules are held by the viral E protein (see Section 1.1) and may be considered as the "key" that the virus uses to open the door that gives it access into the host cell's "lock" or receptor.[56] Equivalent carbohydrate molecules are present on the ZIKV E protein, serving the equivalent function.[66] In both cases, D-mannose and L-fucose moieties that constitute the glycans in the viral E protein are recognised as the main antagonists for DC-SIGN[90], and by knowing and exploring the properties that allow these molecules to fit the DC-SIGN binding site, it may be possible to find a molecule that can mimetise the natural counterparts.
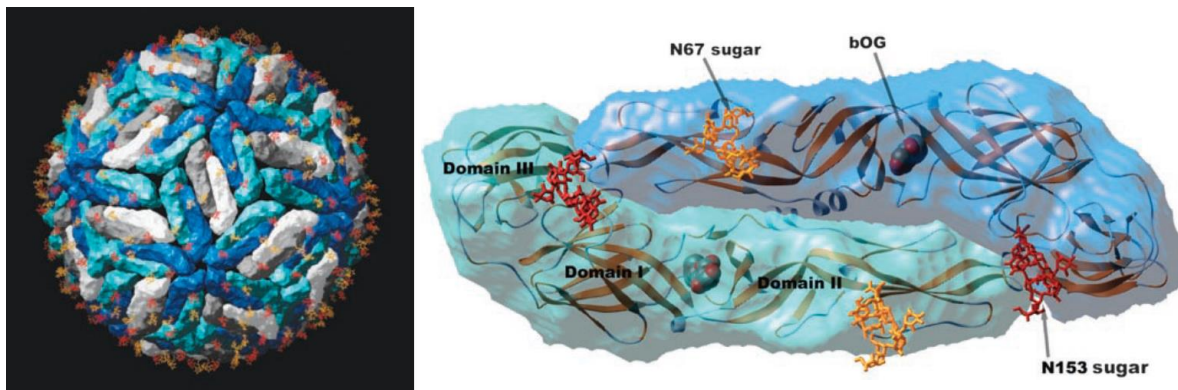
Figure 9 – Carbohydrate distribution on the surface of the DENV particle (left) and semitransparent surface of the DENV E protein (right).[56]

From Fig. 10 it is clear that both D-mannose and L-fucose have a hexane ring, also called pyranoside, as the base structure, differing only in the positioning of the substitutions distributed through the carbon backbone. It is known that both DC-SIGN and langerin interact with these two ligands through substitutions in C3 and C4.[90,92] Taking both the structure of the DC-SIGN binding pocket and the nature of its main antagonists, it is intuitive to understand that potential DC-SIGN antagonists need to have similar characteristics to those of its natural ligands. Such characteristics are groups capable of hydrogen bonding, particularly, hydroxyl groups that need to have a specific placement. Additionally, there is the need for the potential candidate to have a six-vertex ring. Taking this information into consideration, a previous study has pointed out shikimic acid (SA) as having the perfect base structure to fulfil all these requirements.[90]
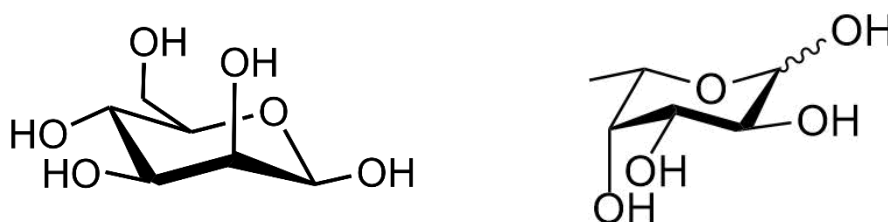
Figure 10 – Structure of the main DC-SIGN ligands, D-mannose (left) and L-fucose (right).

1.3.2.1. Shikimic acid

Deemed the key intermediate in the shikimate pathway, SA, an aromatic carboxylic acid (Fig. 11 a), was named after the plant from which it was first isolated in 1885, the Japanese star anise (*Illicium anisatum*), also known as shikimi (Fig. 11 c).[101,102] SA is produced by plants and microorganisms such as bacteria, fungi and some algae as a lead for aromatic amino acids, including L-phenylalanine, L-tyrosine and L-tryptophan. It is also a precursor for cinnamic acid, flavonoids (anthocyanins, flavones, and tannins)[103,104] and some natural structures such as lignin, the key structural component in the support of tissues in vascular plants.[105,106]
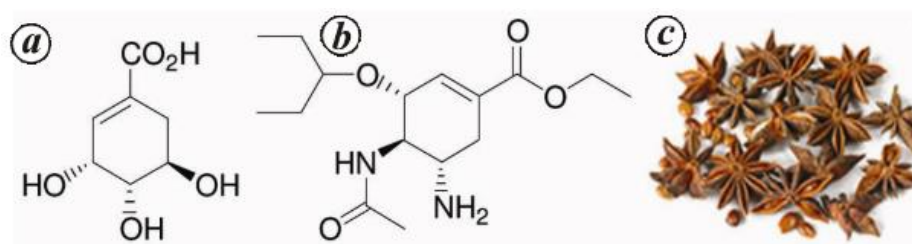
Figure 11 – Structure of (a) SA, (b) oseltamivir and (c) dry Chinese star anise flowers.[107]

Over the years, numerous studies have been performed on SA to understand the potential this molecule holds and as a result many uses have been found. In addition to its biological role, SA has been shown to have antiviral, antibacterial, antifungal and antioxidant properties[104,105]. It has also been shown to act as an antipyretic, anticoagulant, antithrombotic, anti-inflammatory and analgesic.[108] Furthermore, this natural organic compound favours cell renewal and as a result has uses against photo-aging, acne and skin hyperpigmentation.[109] SA has also been used as an additive in hair growth products, and due to its aforementioned antibacterial and antifungal activities it may be used as an anti-dandruff agent.[110] Moreover, SA is used as a precursor for the synthesis of oseltamivir (see Fig. 11 b), the active compound of Tamiflu, the drug used in the treatment of both influenza A and B virus strains.[104–106,108,110,111]

From all the above-described applications, it is clear that SA is highly biocompatible. Additionally, the fact that SA is not a carbohydrate means that it will not be metabolised by the human body.[2] Finally, a few years ago a study showed SA derivatives as being potent hits for inhibiting the DC-SIGN receptor because the positioning of its hydroxyl groups around the aromatic ring provided a great match for interaction with the binding pocket of the receptor.[2] It is on this basis that SA was selected in this work as a potentially suitable ligand that can bind

to DC-SIGN, thus blocking it and preventing the entry of either DENV or ZIKV into the host cell.

1.4. Nanomaterials

According to the European Commission, a nanomaterial is any natural or manufactured material that possesses one or more dimensions in the range of 1 to 100 nm.[112] They appear under the form of wires, particles, clusters, fibres and other intricate structures. Due to their reduced dimensions, such materials exhibit features their bulk counterparts cannot. Examples of these properties are size-tuneable photoluminescence, plasmon resonance, enhanced electrical conductivity, paramagnetism, high surface area-to-size ratio, and others.[113] Additionally, there is a plethora of materials from which nanoparticles (NPs) can be made – metals, polymers, or composites and alloys, meaning there is an extensive list of possible combinations.[114]

In ancient times, NPs were unknowingly employed by the Chinese to stain porcelain in red and towards the middle of the 19th century the first comprehensive study on colloidal gold was published.[115] In the past decade, due to their unique properties, a wide variety of nanomaterials have been developed and investigated and subsequently associated with a myriad of different applications including the biomedical sciences (drug delivery, biomaterials, tissue engineering, imaging, diagnosis and therapy of diseases, biotechnology, etc.)[116], the cosmetics industry (sun screen, skin care products, etc.) agriculture, telecommunications, the materials industry (aerospace science and construction), water purification, catalysis and many more.[117] In the following section, metal NPs and the dendrimer family of nanomaterials will be further discussed.

1.4.1.   Metal NPs

To further deepen the knowledge on the applications of metal NPs, in the past few years, plenty of research has been made about them and reports have shown that they possess antimicrobial (i.e., antibacterial, antifungal and antiviral) activity.[118] This property stems from the fact that metals generally form complexes fairly easily, facilitating their attachment to

membranes, proteins and even the nucleic acid in these small organisms (Fig. 12). Scientists have since found that metal NPs, particularly those composed of noble metals such as silver (Ag) and gold (Au), can attach to and disrupt the membrane of microorganisms thereby compromising its integrity, as well as bind to the proteins and nucleic acid of these organisms thereby impairing them from performing their normal functions.[118] Noble metals are particularly attractive for this task because they are especially resistant to oxidation and the obtention of these metal NPs is extremely easy as they do not require special reaction conditions to be synthesised.[118,119] Additionally, the NPs obtained from these metals tend to be small, which exponentially increases their reactivity and facilitates permeation through microorganism membranes.[120] Apart from Ag and Au, reports exist of magnesium (Mg), titanium (Ti), zinc (Zn) and copper (Cu) oxide NPs being used in the same scope.
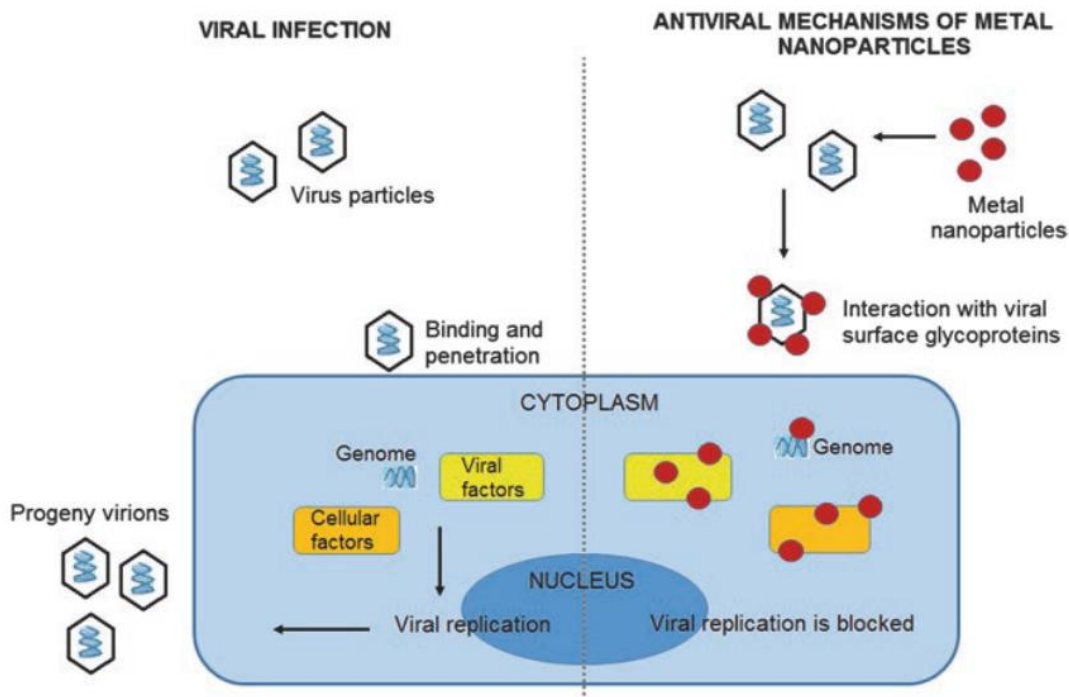
Figure 12 – Antiviral effects of metal NPs and respective mechanism of action as antivirals.[119]

Belonging to the eleventh group and the fourth period of the periodic table, Cu is one of the most abundant and inexpensive metals on Earth. This metal occurs in Nature in the form of several different minerals including chalcopyrite, bornite, malachite, cyprine and many more. Copper appears mostly in two forms, namely the cuprous (+1) and the cupric (+2) forms, and they comprise the oxides, chlorides, sulphides, amongst others. Because this metal never

appears in its pure form naturally, it has to be purified to serve the most various purposes. To do this, the ores containing Cu must undergo smelting followed by refining.[121] After this, it can be used in its pure state or in a variety of alloys used in the production of electronic components such as wires, sheets, or tubes.[122] In human health, Cu is an extremely important micronutrient, as it works as a cofactor for proteins, such as the cytochrome c, which is part of the electron transport chain in the powerhouse of the cell – the mitochondria.[123,124] In fact, Cu is so important that its deficiency has been associated to osteoporosis, a weaker immune system, increased cardiovascular risk, alterations in cholesterol metabolism, and it has also been related to a reduced iron metabolism.[125] For these reasons, according to research, the daily Cu intake for people over the age of 19 is approximately 900 mg.[126] More recently, studies have shown that bulk Cu acts by punching holes in the envelope of viruses, followed by the formation of free radicals that allegedly accelerate its action, and so, it can possibly be used as an alternative to its fellow noble metals. The fact that this mechanism is not virus-specific, makes Cu very suitable to use against most, if not all sorts of viruses.[127,128] Knowing that the properties of metals are further enhanced at the nanoscale and that the reduced size facilitates the action, as evidenced by other noble metal NPs, Cu NPs are very good suitors to target viruses.

1.4.2.   Dendrimers

Dendrimers, from the Greek word "dendron" (tree) and "meros" (part), also known as cascade molecules or arborols,[129] consist of a series of monomers of varying nature that undergo polymerisation to originate their characteristic globular structure. Their discovery and subsequent increase in research all started in the late 1970s to mid 1980s, thanks to the lead work carried out by the research groups of Fritz Vögtle[130] and Donald A. Tomalia[131].

These polymeric materials comprise three main sections, the core, the internal shell, and the outer shell (Fig. 13).[129] They resemble a puzzle made up of several nanoscale pieces (monomers) that are put together to form the jigsaw (dendrimer), with this assembly being repeated cyclically until the desired generation is achieved.[132] Two completely opposite and well-established synthetic methods exist to prepare dendrimers: divergent and convergent. In the divergent method, described by Tomalia et al.[131] and Newkome et al.[133], the molecule starts to be built from the core and grows outwards. In the convergent method, described by Hawker and Fréchet[134], on the other hand, the different dendrons are synthesised individually and are

finally attached together to form the final molecule, and for this reason the growth of the molecule is made from the periphery inwards.[135] Given their difference in nature, both these methods have their qualities and liabilities. The first big difference is that due to its simplicity when compared to the convergent method, the divergent one is believed to be most suitable for large-scale production.[136] In addition, the divergent route provides higher yield than the convergent route, however, this comes at the cost of purity. Finally, the molecules obtained from divergent method are also significantly more prone to defects than the ones obtained from the convergent route.[137]
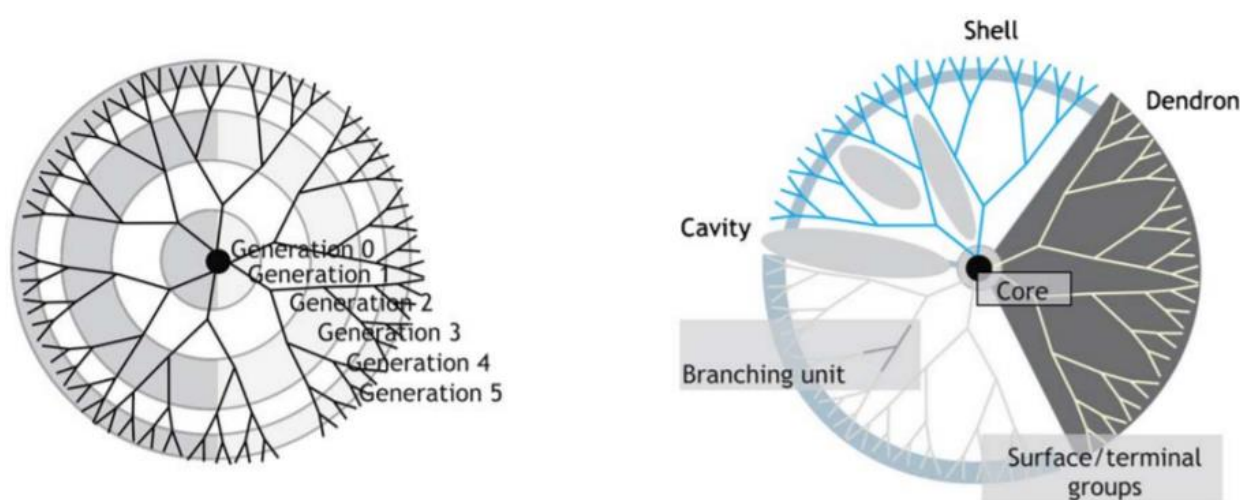
Figure 13 – Schematic representation of dendrimers and how their generations are established (left), as well as the denomination of important terms related to dendrimer nomenclature (right).[138]

In terms of their nature, there are two types of dendrimers, organic and inorganic. Organic dendrimers are simply composed of organic monomers. Contrastingly, inorganic dendrimers that have inorganic atoms in their structure such as silicon or phosphorous, and metallodendrimers that have organic monomers intercalated with metals that can be present either at the core, on branching points, as surface functionalisation or as a mix of some or all of these.[137] This intrinsic versatility makes it possible to fine tune the properties of the final dendrimer molecule, which is particularly important depending on the end goal. For instance, if the dendrimers are intended for biomedical applications, they are expected to be non-toxic and preferably biodegradable.[139] Having this in mind one can choose materials with these properties to build the dendrimers. Furthermore, the number of surface groups on dendrimers that increase with an increase in the generation, gives them unparalleled multivalency, which is especially

useful in receptor targeting.[137] Additionally, because these polymers have a well-defined structure, their molecular mass is also well-defined, which eliminates the problems attached to size polydispersity in the sample and makes characterisation easier.[140] All of these intrinsic characteristics, combined with their increased surface area-to-volume ratio and the ability to functionalise them with virtually any molecule available, is what makes them so appealing for several biomedical applications, such as drug and gene delivery.[129,139,141–143] As a result of extensive research, other applications have also been discovered. These include odontology, tissue regeneration, bioimaging, sensors, catalysis, glycomimetics, the industry of pigments, adhesives, paints and inks, and many, many more.[136,137,141]

1.4.2.1. PAMAM dendrimers

Poly(amidoamine) (PAMAM) dendrimers, shown on Fig. 14, are obtained through the divergent synthetic method, hence why they were coined starburst dendrimers in the early 1980s.[131] Overall, the synthesis of these dendrimers starts with a monomer of ethylene diamine, which serves as a core, followed by addition of methyl acrylate, and this process is followed in loop until the dendrimer reaches the desired generation.[131] They are commercially available in a variety of different generations, typically 1 through 10, with either amine, hydroxyl or carboxyl terminal groups.[139] The availability of these dendrimers with three different terminal groups makes it easier to select which will best suit one's needs. For instance, if the main goal is to use the PAMAM dendrimers in living organisms, it would be best to go either with the carboxyl or hydroxyl groups since they are considerably less cytotoxic than the amine-terminated analogue. However, this inconvenience can be easily bypassed if the surface of the dendrimer is functionalised with a molecule that is harmless to living systems. It is, of course, important to keep in mind that as the generation increases, it gets progressively more difficult to functionalise the PAMAM dendrimers due to steric hindrance issues.[139] To eliminate this issue, the use of lower generations may be best.
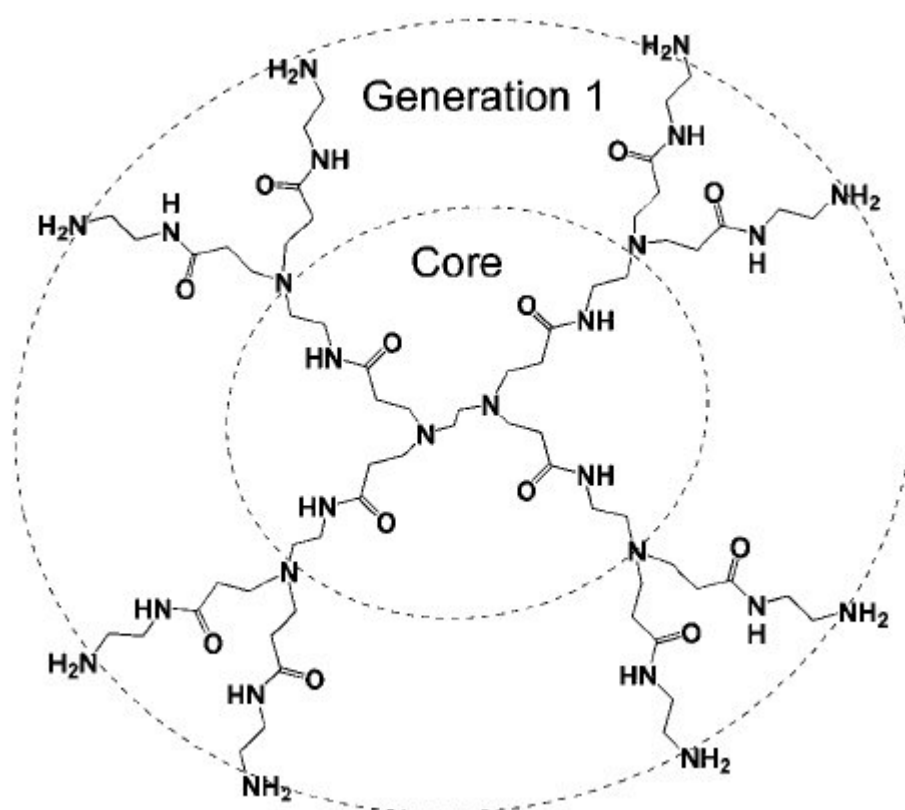
Figure 14 – Representation of generation 1 amine-terminated PAMAM dendrimers.[144]

1.4.2.2. Cu dendrimer entrapped NPs

Since Cu shows higher tendency towards oxidation relative to Ag and Au, especially in the aquatic environment,[122,123] Ag and Au tend to be more widely studied in the field of nanochemistry. However, efforts have been geared towards finding ways to prevent Cu oxidation during the process of synthesis by eliminating oxygen from the reaction environment.[145,146] Another way to do this is by adding a capping agent which will cover the surface of the Cu NPs, preventing oxygen to reach it and oxidise it.[147] In this regard, PAMAM dendrimers have been used as a capping agent to help prevent oxidation of the Cu NPs, as well as to better control their size.[148,149] Several studies exist on the preparation of these so-called Cu dendrimer entrapped NPs (Cu-DENPs), such as electronic devices, catalysts, biomedical research to gauge their antitumoral activity, ability to prevent development of Alzheimer disease and others.[136,146,148–151] Although there have been made some important advances in this area, there is still a lot that is unknown, but considering the aforementioned properties, the future of Cu-DENPs seems to be promising.

1.5. Scope and objectives

An outbreak of dengue in Madeira Island in 2012[8], place where this project was developed, was the primary driving force of the work. In order to minimise the impact of this infectious disease in future outbreaks, as well as zika, the project aimed to design a nanosystem capable of effectively targeting the DC-SIGN receptor that is used by both DENV and ZIKV to infect humans. To attain this objective, the multivalency features provided by the PAMAM dendrimers was combined with the characteristics of a naturally-occurring glycomimetic, SA. Additionally, the antiviral properties of Cu NPs were further added to the developed system as a way to ensure that the final nanosystem not only is capable of blocking the interaction of either virus with the DC-SIGN receptor, but also neutralizing the pathogen. Specifically, generations 4 and 5 of amine-terminated (i.e., $G4.NH_2$ and $G5.NH_2$) PAMAM dendrimers were functionalised with SA via the standard 1-Ethyl-3-(3-dimethylaminopropyl)carbodiimide (EDC)/N-Hydroxysuccinimide (NHS) chemistry. Subsequently, Cu NPs were introduced through chemical reduction using ascorbic acid. All the prepared materials were characterised via Ultraviolet-Visible (UV-Vis) spectroscopy, fluorescence spectroscopy, one-dimensional-Nuclear Magnetic Resonance (1D-NMR), Attenuated Total Reflection-Fourier Transform Infrared (ATR-FTIR), Dynamic Light Scattering (DLS), Inductively Coupled Plasma Optical Emission Spectroscopy (ICP-OES), and Scanning Electron Microscopy (SEM). Finally, some of the developed complexes were evaluated for cytotoxicity towards HEK 293T cells.

CHAPTER 2 – METHODOLOGY

The experimental work may be divided into four sections. In the first section, the focus is directed towards the coupling of SA with two different generations of the PAMAM dendrimers. The second part involves the reduction of Cu onto the previously synthesised conjugates, while the third section entails the characterisation of all the starting reagents, as well as the synthesised complexes, via DLS, fluorescence spectroscopy, ATR-FTIR, ^{1}H NMR, SEM and ICP-OES. Lastly, the influence of the prepared complexes on cell viability, namely on HEK 293T cells, was evaluated.

2.1. Materials and reagents

Generations 4 and 5 of PAMAM dendrimers with amine termini in methanol were obtained from Dendritech® Inc (MI, USA). Other reagents used include SA (Acros organics; Leicestershire, UK), NHS (Aldrich, USA), EDC (Sigma Aldrich, USA), copper sulphate pentahydrate (Riedel-de Haën, Seelze, Germany) and ascorbic acid (Merck, Germany). Dialysis membrane with a molecular weight cut-off (MWCO) of 10kDa (Spectrum laboratories, New Jersey, USA) and centrifugal filter Amicon Ultra-15 with a MWCO of 3kDa (Merck Millipore, Darmstadt) were also used. Dulbeco's Modified Medium (DMEM), Fetal Bovine Serum (FBS), antibiotic/antimycotic solution (100X), collagen (collagen I rat protein, tail) and trypsin-ethylenediaminetetraacetic acid (trypsin-EDTA, 0.25%) were acquired from Gibco (Thermo Fisher, USA). Resazurin was obtained from Merck (Germany).

2.2. Synthesis of SA-functionalised PAMAM dendrimers

In this section, the methodology to attach SA to either G4.NH$_2$ or G5.NH$_2$ PAMAM dendrimers via EDC/NHS coupling is described. The reaction, represented in a simplified way in Fig. 15, comprised two steps, namely activation and then coupling.
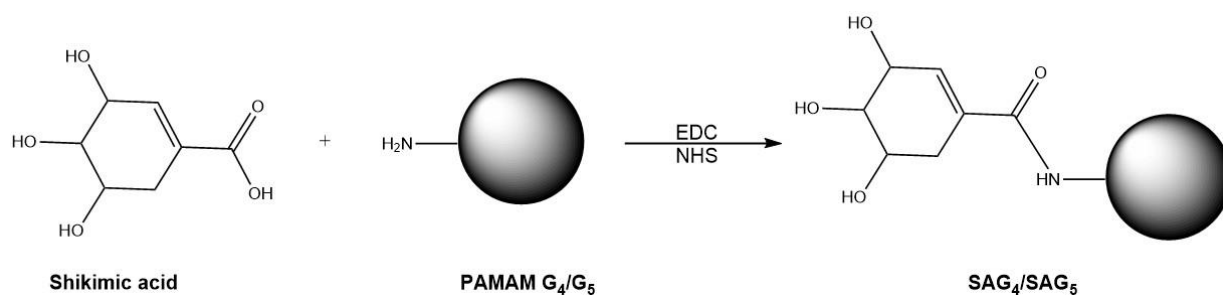
Figure 15 – Simplified mechanism of EDC/NHS coupling between amine-terminated PAMAM dendrimer and SA.

In the first step, the SA ligand was mixed with a 5 molar excess of EDC and a 10 molar excess of NHS in the same order. After a 4h activation period, the dendrimer was added in a dropwise fashion so that the dendrimer-to-ligand ratio was 1:96 and 1:192 for $G4.NH_2$ and $G5.NH_2$, respectively. The reaction mix was left to react for another 4h after which, the complexes were purified via dialysis against distilled water for 3 days in order to remove any urea, uncoupled ligand, unreacted reagents and other by-products. Finally, the complexes (hereon referred to as SAGx, where x indicates the generation) were freeze-dried and characterised via DLS, UV-Vis, fluorescence spectroscopy, ATR-FTIR, ^{1}H NMR and SEM.

It is important to note that both dendrimer generations were purified beforehand via dialysis using the same conditions used to purify the complexes in order to remove the methanol in which they were stored. They were then freeze-dried and stored at -20ºC until they were deemed ready for use.

2.3. Synthesis of SA-PAMAM encapsulated Cu NPs

The procedure described in this section is a result of the adaptation of studies that have already been made in the past.[148,149,152,153] With the intent of encapsulating Cu NPs into the previously synthesised conjugates as depicted in Fig. 16, an aqueous solution of copper II sulphate pentahydrate was prepared and its pH changed to 5.7. Subsequently, this solution was added in a dropwise fashion to an aqueous solution of each respective SA-dendrimer conjugate, such that there was a molar excess of copper sulphate (16:1 of $SA:G4.NH_2$ and 32:1 of SA:G5). Notice that this step caused the colour of the solution to shift from transparent to a dark blue

upon addition. The solution was stirred for 30 minutes to ensure the Cu^{2+} ions had been successfully coordinated to the tertiary amines in dendrimer.[148]

Thereafter, an aqueous solution of ascorbic acid (AA), a mild reducing agent, was prepared to a pH of 7.00 and was added to the SA-dendrimer conjugate solution of interest (100 molar excess to Cu), making the reaction mixture shift colour to a yellow tone. The solution was left to react at 60°C for 4h and the final product was then purified using centrifugation (4000 *g* for 30 minutes) in a centrifugal membrane. From this purification step, two fractions were obtained – one containing the complex (CuSAGx) and another bearing the impurities (CuSAGx imp). To complete the purification process, the samples were freeze-dried and characterised via ^{1}H-NMR, ATR-FTIR, fluorescence spectroscopy and DLS.
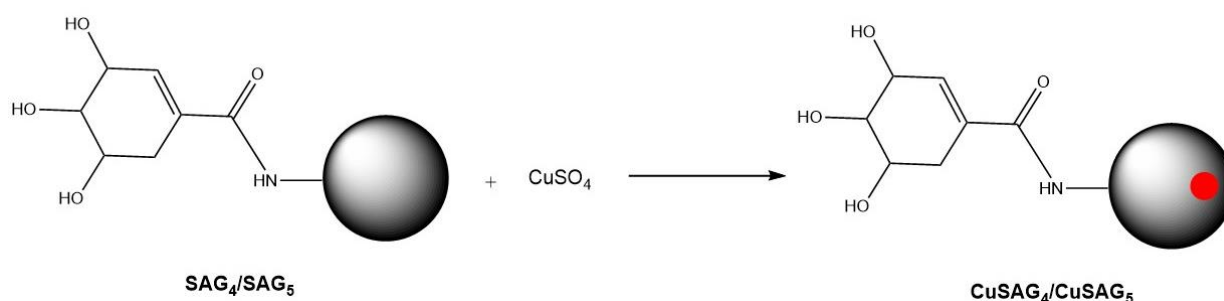
Figure 16 – Simplified mechanism of encapsulation of CuNPs in the SAGx complexes.

2.4. Characterisation

In order to determine if the EDC/NHS coupling process was successful, as well as Cu entrapment, a series of techniques was used to characterise the SA-functionalised PAMAM dendrimers and the respective Cu DENPs. For structural analysis, UV-Vis, ATR-FTIR, ^{1}H-NMR and fluorescence spectroscopy were performed. To determine the hydrodynamic radius of the samples, DLS was used. In addition, the Zp was also determined and the morphology of the dry samples was observed through SEM, and the content of Cu was detected via energy dispersive X-ray (EDX) spectroscopy and ICP-OES.

Before characterisation, all samples underwent purification and were subsequently freeze-dried and stored at 5°C. Depending on the demands of the characterisation technique the

samples were then either dissolved in a suitable solvent or used in their dry form. Sample characterisation then took place as explained in the following sections.

2.4.1. UV-Vis spectroscopy

The absorption in UV-Vis originates from chromophores – groups with high electron density such as double bonds and electronegative elements. For this reason, this technique is widely used to study a wide variety of organic molecules.[154] Since, as reported by previous studies, Cu NPs exhibit a characteristic exponential-like curve towards lower wavelengths, this technique was used to detect the existence of such particles.[148]

To characterise the SA-functionalised PAMAM dendrimers and the respective Cu DENPs via UV-Vis spectroscopy (Perkin Elmer, Lambda 25), aqueous solutions (in ultrapure water – UP H_2O) of all compounds were prepared as indicated in Table 1.

Table 1 – Summary of the concentrations used for every sample prepared in UP H_2O analysed through UV-Vis spectroscopy.

Compound	Concentration
SA	10 µg/ml
AA	10 µg/ml
CuSO₄	0.1 M
Gx.NH₂	2 mg/ml
SAGx and CuSAGx	1 µg/ml

2.4.2.   Fluorescence spectroscopy

Much like UV-Vis spectroscopy, photoluminescence can also provide valuable information about the electronic structures of molecules.[115] In the specific case of nanomaterials, this is an especially important technique since nanoscale materials can be used as fluorescent sensors for many applications.[155]

In order to determine whether or not the compounds prepared in this study displayed photoluminescence, fluorescence spectroscopy (Perkin Elmer, LS 55) was employed. Freshly prepared solutions of the starting reagents, as well as the SA-functionalised PAMAM dendrimers and the respective Cu DENPs, were prepared in UP H_2O at a concentration of 2 mg/ml. The excitation and emission slits used were 15 and 5 nm, respectively and the excitation wavelength was 390 nm.

2.4.3.   ATR-FTIR spectroscopy

In FTIR, there are two types of absorptions that arise from molecules – stretching and bending vibration bands. Typically the former occurs at higher wavelengths than the latter.[154] Usually, when looking at the FTIR spectrum of any compound, attention should be turned towards finding the absorption bands arising from the bond stretching of certain groups.[154] When the compounds used are known, there is the need to look for the peaks that originate from the stretching vibrations of each characteristic type of group the molecule under analysis bears.

For FTIR characterisation, an ATR device (DurasamplIR II, Smiths Detection) was adapted to the FTIR equipment (Perkin Elmer, Spectrum Two) where the dry samples were then placed over its diamond crystal. The samples were scanned for 36 runs in a range of 4000 – 650 cm^{-1}. To perform the analysis, approximately 5 mg of each compound were used.

2.4.4. NMR spectroscopy

NMR spectroscopy is widely used in medicine for diagnostic imaging, engineering and material testing, as well as in scientific research to obtain in-depth information about numerous molecules and to follow the progression of chemical reactions.[156] Relative to ^{13}C NMR, ^{1}H NMR provides a considerable amount of information about a molecules structure and any changes that may occur within it.[154] When combined with FTIR, NMR makes it possible to more efficiently determine the structure of the molecules. Hence these two techniques being known as power tools in structural analysis.[157]

Here, all the samples assessed (approximately 5 mg) were dissolved in 500 µl deuterated water (D_2O, δ = 7.490) and were analysed with a 400 MHz pulse (Bruker NMR Spectrometer, UltraShield™ 400 Plus, console: Avance 400 II+). Data acquisition and treatment were performed using the TOPSPIN Software (version 4.0.6) and all the acquired spectra were calibrated relative to the residual solvent peak.

2.4.5. DLS

In the current scope of science, more specifically, the nanomedicine field, DLS is a tool of utmost importance in collecting information on the size of nanomaterials.[158]

DLS, as the acronym indicates, relies on the principle that all particles, regardless of their size, scatter light. Information given by the scattered light is collected and is combined with the random movement exhibited by the particles in suspension (i.e., Brownian motion) to in turn provide the hydrodynamic radius of the particles.[158]

For all DLS analyses performed in this study, all the starting reagents and the products were prepared in water to a final concentration of 0.5 mg/ml, and were then filtered using a 0.2 µm pore filter. The DLS data, obtained using a Zetasizer Nano ZS (Malvern Instruments Ltd.), were acquired in triplicate with each run being performed for 40s. The parameter that was taken into account here was the mean hydrodynamic radius (Z-average).

2.4.6. SEM coupled with EDX spectroscopy

As a surface analysis technique, SEM is widely used in the field of materials sciences, biology, biomedicine and many others. This technique provides invaluable information about the topography, chemical composition and crystalline structure of samples and is widely used in the characterisation of Cu NPs.[159,160] It is also usually combined with EDX analysis to give complementary data about chemical composition.[161]

For SEM/EDX analysis, a Bench SEM (Phenom - ProX) using the ProSuite image acquisition, processing, and analysis Software was implemented. All freeze-dried samples were placed and pressed over carbon adhesive for better fixation. In order to eliminate possible debris that could be detached from the sample into the microscope chamber during analysis, the holders were dusted off with compressed air. Since all samples needed to undergo EDX analysis and Cu was the main element that was being searched within the analysis, to avoid interference, carbon adhesive was used instead of the Cu option. Two types of holders were used: (1) charge reduction for the non-conductive SAGx samples so as not to degrade the material and (2) a standard one for the conductive CuSAGx samples. The SEM images were obtained and the EDX analyses was performed under an accelerated voltage of 15 kV, in order to identify the weight percentages (wt. %) of Cu in the samples.

2.4.7. ICP–OES

When exposed to high energy levels, atoms transition into excited states. If the energy employed is high enough, dissociative ionisation and collisional excitation can take place. Based on this principle, ICP-OES, also known as inductively coupled plasma – atomic emission spectroscopy (ICP-AES), heats the samples using incredibly high temperatures (8000 – 10000 K). The energy decay at specific wavelengths, which depends on the element that is being analysed, is then used to determine the concentration of the said elements in the samples. In the specific case of ICP-OES, at least three spectral lines are considered in order to ensure that the emission that is being analysed is indeed from the element of interest.[162]

In order determine the percentage of Cu in the Cu-containing SA-functionalised PAMAM dendrimers, ICP-OES was performed using a Perkin Elmer Optima 2000 DV at the

Laboratório de Análises do Instituto Superior Técnico (LAIST, Lisbon, Portugal). To eliminate the organic matrix of the freeze-dried samples and get them ready for analysis, calcination (at 550ºC) in platinum crucibles was performed, followed by acid digestion in nitric acid.

2.5. Cytotoxicity studies

Cell culture studies play a role of paramount importance in evaluating the effect of different compounds on tissues or organs. In this work, the cytotoxic effects of the prepared compounds were evaluated using the human embryonic kidney cell line (HEK 293T; ATCC® CRL-3216™).

Before exposing the cells to the test compounds, solutions were prepared. According to a previous study performed using HEK 293T cells, SA shows an IC_{50} (half maximal inhibitory concentration) of 1 mM.[163] For this reason, the stock solution for SA was prepared at a concentration of 10 mM. Stock solutions of both the $G4.NH_2$ and $G5.NH_2$ PAMAM dendrimers (2 μM)[164] and the equivalent SA-functionalised dendrimers (5 mM) were also prepared. The dendrimer solutions were diluted to concentrations of 0.1 and 1 mM, while the SA-functionalised dendrimers were diluted to concentrations of 0.01, 0.05, 0.1, 0.5, 1, 2 and 4 mM. Note that all the compounds were diluted in water purified by a Millipore Water Purification system, and sample preparation was performed in a laminar flow chamber to preserve sterility as much as possible. For detailed information on the working concentrations for all compounds, refer to table 2.

Table 2 – List of concentrations used for all the compounds used in the cytotoxicity assays.

Compound	Concentration in the well
SA	1 mM
Gx	0.01, 0.1, 0.2 mM
SAGx	0.001, 0.005, 0.01, 0.05, 0.1, 0.2, 0.4, 0.5 mM

The HEK 293T cells were proliferated in 10 cm petri dishes under incubation under the standard conditions (5% CO_2 and 37°C) until the confluence reached nearly 80-90%. DMEM supplemented with 10% FBS and 1% antibiotic/antimycotic was used in all experiments. Cells were detached using trypsin, stained and then counted. Thereafter a fresh cell suspension was prepared and the cells were distributed into 96-well plates pre-treated with collagen type I (0.2 mg/ml in 0.25% acetic acid). In each case, 5000 cells/well was taken into account. The cells were then incubated for 24h, after which the compounds were added. The cells were finally incubated for another 48h. Note that each sample concentration and the controls were tested in quadruplicate and each assay was repeated 3 times to ensure reproducibility.

The 100% viability control consisted of cells in 200 µl of medium, while the solvent control consisted of 20 µl of ultrapure water mixed with 180 µl of medium. For the samples tested, a mix of 180 µl of medium and 20 µl compound solution was used such that the final test concentration was obtained.

2.5.1.   Resazurin assay

The resazurin assay is a widely used cell viability test in which resazurin is reduced to resofurin.[165] After the 48h exposure of the cells to the test compounds, the existing medium was removed and subsequently substituted with a solution of 10% resazurin in DMEM. The plates were then incubated for 4h, after which 100 µl of the solution in each well were transferred to a white 96-well plate. A well with the resazurin solution (blank) was also included. The fluorescence was finally read in a microplate reader (Perkin Elmer, Victor 3) using an excitation wavelength of 530 nm and an emission wavelength of 590 nm.

CHAPTER 3 – RESULTS AND DISCUSSION

In this section, the results from the characterisation and cytotoxicity studies of the prepared SA-functionalised PAMAM dendrimers and their corresponding Cu DENPs is presented. Although the synthesis of the SAGx and CuSAGx samples entailed two separate steps, the results are compiled together.

3.1. Physical aspect of the SA-functionalised PAMAM dendrimers and respective Cu DENPs

The first step in the preparation of the Cu DENPs involved the conjugation of SA to either the $G4.NH_2$ or the $G5.NH_2$ PAMAM dendrimers using EDC/NHS coupling chemistry. The freeze-dried SAGx samples were observed to have a highly different texture to them (see Fig. 17). While the SAG4 conjugate had a cotton-like consistency, SAG5 had a crystal-like appearance.

Figure 17 – Comparison of the physical aspect between SAG4 (left) and SAG5 (right).

As Fig. 18 shows, after the second reaction step in which Cu was reduced to obtain CuSAGx conjugates, a purplish deposit on the bottom of the flask was observed, indicating that the majority of the Cu that was added to the reaction mixture reacted outside of the dendrimer and accumulated at the bottom. Although the reaction mixture was left to react for nearly 30 minutes so that the Cu could permeate the dendrimer shell, the existence of the aforementioned deposit suggests that Cu entrapment in the dendrimer scaffold may have been unsuccessful. It is possible that due to the architecture of the amine-terminated PAMAM dendrimers, the Cu ions have a higher tendency to coordinate to the terminal amines causing the ions to be

coordinated in the outer shell of the dendrimer rather than permeating further in it.[148,166] Furthermore, it has been stated in previous studies that H^+ competes with Cu^{2+} in tertiary amine groups, which further corroborates the idea that it may be difficult to keep the ions inside the dendrimer, especially in solvents like water.[149]

Figure 18 – Colour comparison of the CuSAG4 (left) and CuSAG5 (right) complexes after synthesis.

After freeze-drying the complexes obtained from the second reaction step, yellowish brown powders were observed (Fig. 19), contrastingly to the respective SA-functionalised PAMAM dendrimers. At the same time, the purification extracts (hereon referred to as CuSAGx imp) obtained after ultrafiltration of the samples, had the same colour, which may indicate that the colour originated from the Cu NPs that were not attached to PAMAM.[153]

Figure 19 – Comparison of the physical aspect between CuSAG4 (right) and CuSAG5 (left).

3.2. Characterisation of the SA-functionalised PAMAM dendrimers and respective Cu DENPs

3.2.1. UV-Vis spectroscopy analysis

The UV-Vis spectra obtained for the starting materials, the SA-functionalised PAMAM dendrimers and their respective Cu DENPs are shown in Fig. 20. It is possible to observe that SA shows an absorption band with a maximum around 201 nm versus the 212 nm reported in the literature.[167] According to previous research, when dissolved in water, AA is known to have an absorption band at around 265 nm which arises due to the presence of conjugated double bonds.[168] Looking at Fig. 20, it is possible to see that, similarly to what has been reported, AA exhibits a maximum absorption at 263 nm.[169] Finally, when using pH values above 3.5, the tertiary amines in the PAMAM dendrimers are deprotonated, and for this reason, they exhibit an absorption peak in the range of 280 – 285 nm.[170] Looking at Fig. 20, no peak is observed for each PAMAM dendrimer in this range indicating that the pH may have been too acidic for it to appear. When assessing the SAGx complexes, it is clear that they exhibit UV-Vis spectra equivalent to their counterparts (i.e., SA and PAMAM).
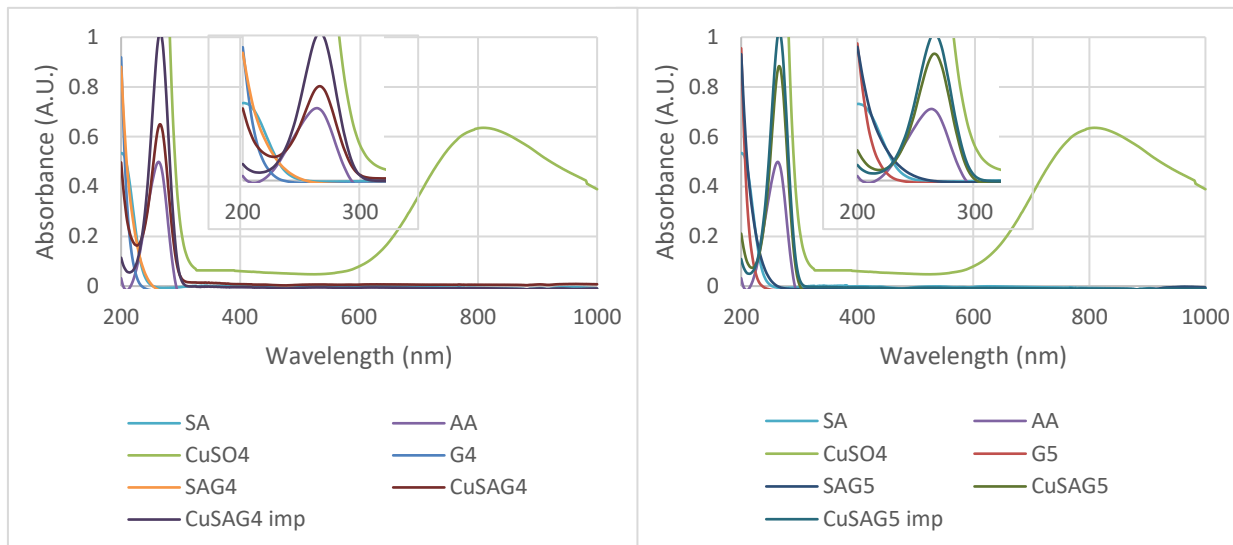
Figure 20 – UV-vis spectra of the all the starting reagents (SA, AA, CuSO4, Gx) used for the synthesis of generation 4 (left) and 5 (right) complexes and final products of steps one (SAGx) and two (CuSAGx). A sample concentration of 10 µg/ml was prepared for SA and AA, while the CuSO4 concentration was 0.1 M. For Gx, a 2 mg/ml sample concentration was used and for both SAGx and CuSAGx sample concentrations of 1 µg/ml were prepared in UP H_2O.

CuSO4 starting reagent was also assessed. Once dissolved in water, CuSO4 quickly turns into $[Cu(H_2O)_6]^{2+}$, a coordination complex that has a blue colour and in this form presents an absorption maximum at around 800 nm in the spectrum of light (see Fig. 20), which represents the d-d transitions for Cu^{2+}.[149,171] In addition, it also has charge-transfer bands at the opposite end of the spectrum, typically in the range of 200 and 300 nm,[123] which again is evident in Fig. 20. In the past, PAMAM-encapsulated CuNPs have been reported to have an exponential-like profile towards smaller wavelengths (typically 200 nm).[171] However, this was not observed here (see Fig. 20). Furthermore, the absence of the plasmon resonance band that usually appears at 570 nm[148] reinforces the idea that the expected material is not in the system. Alternatively, this may indicate that the nanoparticles are smaller than 5 nm in diameter, or that the amount of Cu in the complex was too low to be detected using this technique.[148] Instead, the samples exhibited a band centered around 263 nm, which, as already established, corresponds to the absorption of AA, indicating that the purification step did not remove it completely. This is further reinforced by the presence of this same band in the spectra of the impurity extracts (i.e., CuSAGx imp).

3.2.2. Fluorescence spectroscopy analysis

From the spectra presented in Fig. 21, it is evident that upon excitation at 390 nm, only the $CuSAG_4$ complex and the $CuSAG_5$ imp exhibit fluorescence with an emission at ~455 nm. At the chosen excitation wavelength, neither SA nor AA presented emission. Unlike these acids, the dendrimer showed some fluorescence, at around 450 nm, which is in line with what has been previously reported.[172]

Regarding the first reaction step, the prepared SA-functionalised PAMAM dendrimers (i.e., SAGx) did not show fluorescence. However, this changed with the second reaction step where both the two CuSAGx complexes and CuSAGx imp showed emission at ~455 nm, even if faint. In the case of CuSAG4, it is visible that the corresponding impurities sample show little to no fluorescence, however, the situation is reversed in the case of the CuSAG5 synthesis, where the impurities (i.e., CuSAG5 imp) obtained from purification show a clearly higher fluorescence than the target complex (i.e., CuSAG5). This suggests that the by-products, potentially the conjugation of Cu and AA, are responsible for the obtained fluorescence.

Depending on their size, Cu NPs have been shown to exhibit fluorescence maxima at wavelengths below 330 nm,[155] however, that was not what was obtained. Regardless, although the obtained fluorescence was not caused by CuSAGx samples, the presence of Cu really did contribute for this phenomenon and this can be a matter of tuning the reaction's conditions to hopefully lead to the desired product.
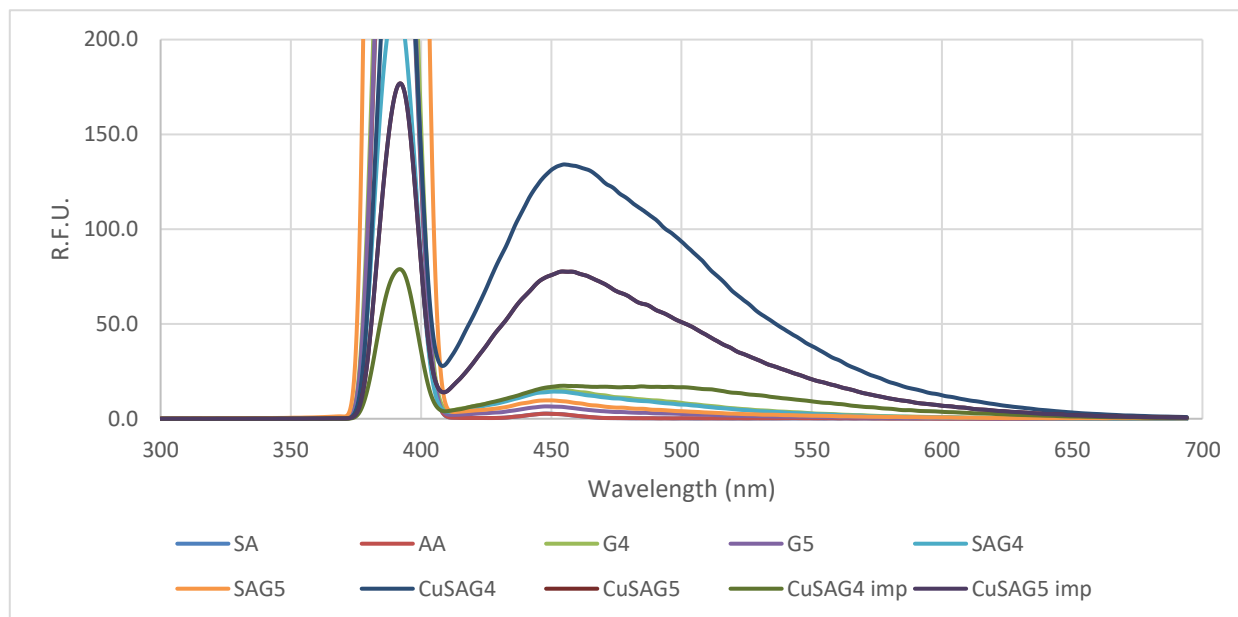
Figure 21 – Fluorescence spectra of solutions of the starting reagents, SA, AA, G4.NH$_2$ and G5.NH$_2$, the SA-functionalised PAMAM dendrimers (SAGx) and the respective Cu DENPs (CuSAGx). In each case, a sample concentration of 2 mg/ml was in prepared in UP H$_2$O. The excitation wavelength was 390 nm and the excitation and emission slit widths were 15 and 5 nm, respectively.

3.2.3. ATR-FTIR spectroscopy analysis

For this part of the work, FTIR spectroscopy was used to assess if there were any significant changes in the G4.NH$_2$ and the G5.NH$_2$ PAMAM dendrimer after the two different reaction steps. Fig. 22 shows the FTIR spectra obtained for each PAMAM dendrimer, SA, AA, each SA-functionalised PAMAM dendrimer and each respective Cu DENP. To better understand the FTIR analysis, the structures of the organic molecules used to obtain the complexes are presented in Fig. 23. Since these compounds are widely known and extensively studied, the analysis presented in this section concentrates on the confirmation of the most important peaks.
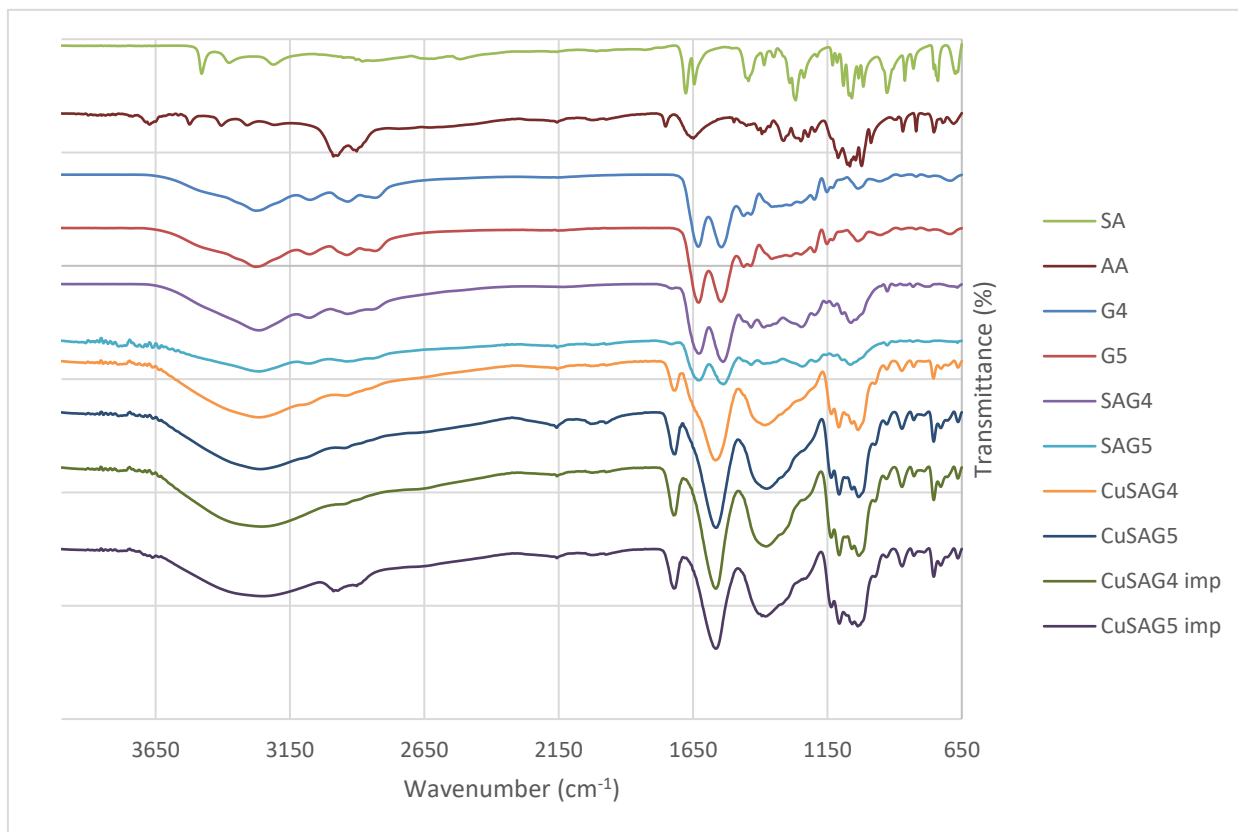
Figure 22 - ATR-FTIR spectra of the SA-functionalized PAMAM dendrimers (SAGx), the Cu DENPs (CuSAGx) and the starting reagents, SA, AA, G4.NH$_2$ and G5.NH$_2$.
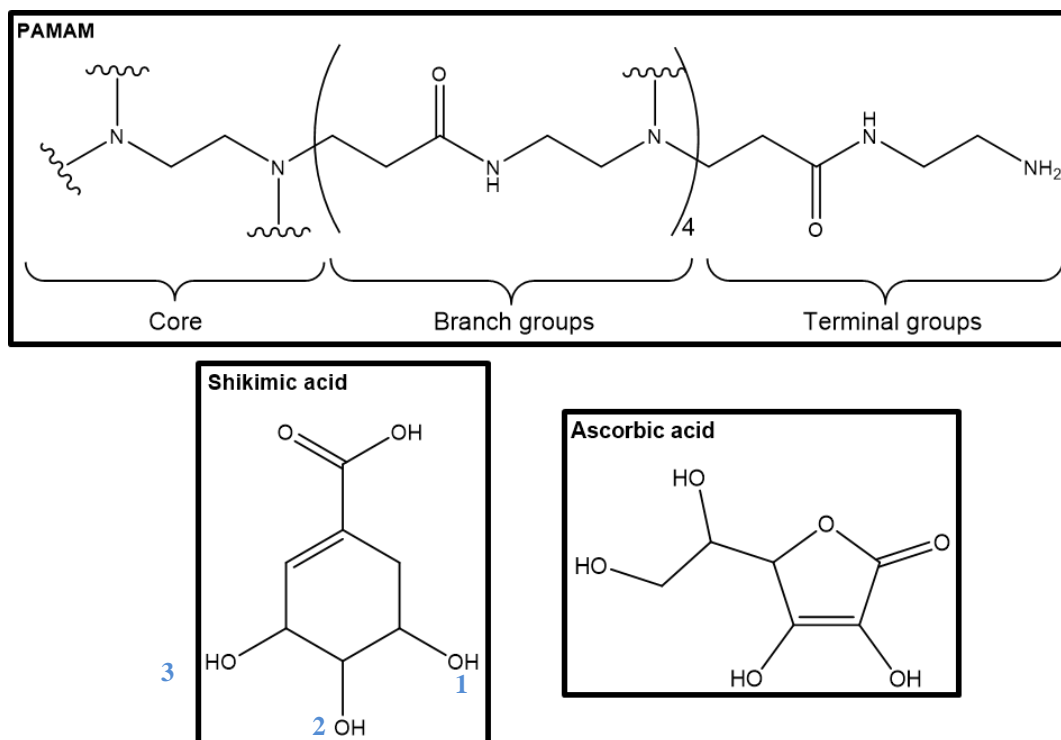
Figure 23 – Molecular structures of the SA-functionalized PAMAM dendrimers (SAGx), Cu DENPs (CuSAGx) and the starting reagents, SA, AA, G4.NH$_2$ and G5.NH$_2$.

Since SA is a cyclic carboxylic acid with a double bond in the ring (see Fig. 22), the bands one is looking for refer to the stretching of the carboxyl and hydroxyl groups, C=C stretch and C-H groups, where the carbon partakes in a sp^2 bond. Additionally, SA possesses three extra hydroxyl groups bound to three of the carbons in the hexane ring. As seen in Fig. 23, SA has 4 hydroxyl groups, 3 of which are visible in the FTIR spectrum. These groups appear at 3475 cm^{-1}, 3380 cm^{-1} and 3210 cm^{-1}. Furthermore, in this carboxylic acid, the C=O stretch vibration arises at 1680 cm^{-1}. Additionally, there is the presence of a C=C bond which can be seen at 1640 cm^{-1}. All this obtained data is in line with previous reports.[173]

The structure of AA consists of a tetrasubsituted lactone ring (see Fig. 23). These substitutions include an aliphatic chain, a carboxyl group and two hydroxyl groups. Similarly to what happens in the case of SA, all the OH groups are represented in the spectrum (3670 cm^{-1}, 3520 cm^{-1}, 3410 cm^{-1} and 3310 cm^{-1}). The carboxyl group regarding the ketone function appears at 1750 cm^{-1}. In addition, the ring also possesses a double bond which has its stretching vibration band at 1650 cm^{-1} and as a result of it, the stretching vibration band of C-H in sp^2 hybridization should appear, but that is not the case due to the presence of a conjugated system.[154] Once more, all data are according to the references.[174]

PAMAM dendrimers have a unique basic structure that is repeated as the generation increases. For this reason, and according to the theory behind the FTIR technique, this molecule has the same FTIR fingerprint regardless of the generation. This can be seen in Fig. 22, where both generations have the same spectrum profile. The dendrimer has both primary and secondary amines, which can be seen at around 3300 cm^{-1}. The broad nature of this band suggests the presence of solvation water molecules.[154] Related to this group, there is also the bending stretch of the N-H bond that can be seen at 1550 cm^{-1}. Furthermore, the C=O stretching vibration occurs at 1630 cm^{-1} and as reported by others, this band partially overlaps with the previous.[154] Unlike the previous compounds, the PAMAM dendrimers do not have C=C bonds and for this reason only the C-H stretch vibration that shows up refers to sp^3 hybridisation, which shows up below 3000 cm^{-1}. These results are in accordance with the consulted bibliography.[175]

Regarding the two different SAGx complexes, it is clear from Fig. 22 that overall their profiles resemble that of the dendrimers. Also, because the bands referring to the hydroxyl groups in the carboxylic acid appear at the same range of the bands characteristic of the presence

of primary and secondary amines in the dendrimer, they end up overlapping. In the same manner, the bands referring to both C=O and C=C from both compounds are overlapped in the spectrum of the resulting complexes. Taking this into consideration, it is safe to say that FTIR is not the best technique to ensure that the first step of the synthesis was successful.

Comparing the spectra of the compounds obtained in steps one and two of the synthesis, it is noticeable that after Cu reduction, there are minor differences in the spectrum, aside from the presence of the ketone group stretch band that arises from the presence of AA in the CuSAGx samples (see Fig. 22). This suggests that the purification step did not completely remove AA from the complexes. In addition, comparing these spectra with the ones obtained for the CuSAGx imp. samples, it is clearly visible that there is little to no difference in the profile, which reinforces the idea that this technique is not the best to detect if the reaction was successful.

3.2.4.   NMR spectroscopy analysis

In this work, the NMR technique was used to estimate the degree of functionalisation of the terminal groups of the G4.NH$_2$ and G5.NH$_2$ PAMAM dendrimers with SA. For this, the spectra of the starting reagents and the SAGx reaction products were acquired by ^{1}H NMR and finally compared. All the chemical shifts mentioned in this section and respective signal attribution can be found in the annexes section at the end (tables 5 through 9). In the specific case of ^{1}H NMR, signal multiplicity, well described by the spin-spin splitting rule, depends on the amount of chemically equivalent protons in the vicinity.[154]

Based on the chemical structure presented in Fig. 24A as well as in Fig. 25A, it is visible that SA has a total of 6 protons bound to its carbon backbone and 4 additional ones provided by the hydroxyl groups. In each case, it was possible to attribute the six signals in the ^{1}H NMR spectrum of SA to all six protons in the carbon backbone. Proton types <u>a</u> and <u>b</u> indicated in the SA structure correspond to the equivalently identified signals in the spectrum at lower shifts (i.e., at 2.201 and 2.718 ppm). Proton types <u>c</u>, <u>d</u> and <u>e</u> in SA, corresponding to 3.768, 4.019 and 4.460 ppm in the ^{1}H NMR spectrum, respectively, are the ones sharing a carbon with a hydroxyl group and their proximity to the double bond increases the chemical shift at which they appear. Lastly, the signal at a lower chemical shift (i.e., at 6.831 ppm) is the one that is heavily

influenced by the highly electronegative components of the molecule, the 3 hydroxyl groups and the double bond itself, followed by the carboxyl group. These results are in accordance with previous studies.[111]

In the case of AA, it possesses a total of 8 protons, 4 of which are part of the hydroxyl groups and the other 4 being attached to the carbon backbone (see the AA chemical structure in Fig. 24B and Fig. 25B). The signal in the ^{1}H NMR spectrum of AA at 3.712 ppm corresponds to two protons (g), because it is the farthest from the high electronegative density of the molecule (ketone group and ring double bond). The signal immediately after at 4.051 ppm corresponds to proton type h and is originated by one proton, while the signal at 4.959 ppm can be attributed to proton type i. Once again, these results are in line with previous reports.[176]

The signal attribution for the ^{1}H NMR spectra obtained for both the G4.NH$_2$ and G5.NH$_2$ PAMAM dendrimers was an adaptation of a previous study.[177] According to the study and, looking at the chemical structure depicted in both Fig. 24C and Fig. 25C, and because they are symmetrical, PAMAM dendrimers have 4 different proton types. The signals l and k refer to protons that are between two highly electronegative atoms, which is the case of oxygen and nitrogen that naturally pull electronic density towards each other and in this situation end up cancelling each other's effect, which results in these protons having similar behaviour as they would if they were only surrounded by the standard alkyl groups. However, since the l protons neighbour a sp^2 bond and an oxygen, it makes sense they are at a higher chemical shift than the k protons. The protons in the core (i.e., signal j) are between two electronegative yet identical atoms (i.e., nitrogen) that slightly shift their signal towards higher chemical shifts. To the same group of protons belong those right before each branching point which are in a similar environment to those in the core. Finally, the protons responsible for the m signal not only belong to the carbon atom that directly binds to a highly electronegative atom such as nitrogen, but they also neighbour the double bond and yet another highly electronegative element, the oxygen atom. These four proton types could be associated with the four main signals in the ^{1}H NMR spectrum obtained for each molecule (see Fig. 24C and Fig. 25C). In each case, the signals were integrated and the sum of the integrals (see table 7 in annex section) was set to the total number of protons in each case. This calculation originated the number of protons that produced every single signal in the spectrum. In the G4.NH$_2$ PAMAM dendrimer the k signal at 2.409 ppm in Fig. 24C corresponds to 251 protons, while the equivalent signal in G5.NH$_2$ PAMAM

shown in Fig. 25C counts with 498 protons. The signal arising from proton type i at 2.603 ppm represents 131 and 263 protons for G4.NH$_2$ and G5.NH$_2$, respectively. Signal l at 2.759 ppm in Figs. 23C and 24C, on the other hand, represents 361 protons in a G4.NH$_2$ molecule and 738 protons in a G5.NH$_2$ molecule. Finally, signal m at 3.221 ppm in each ^{1}H NMR spectrum corresponds to 254 and 520 protons for G4.NH$_2$ and G5.NH$_2$, respectively.

Finally, the success of the coupling reaction of SA with the PAMAM dendrimer of interest was assessed. For this, the spectrum of each starting reagent (i.e., SA and Gx) was compared to the spectrum of the final product of interest (i.e., SAGx). Overall, it is possible to see in Fig, 24A, 24C and 24D, as well as in Fig. 25A, 25C and 25D, that only one of the signals stemming from SA (b) overlapped with the one of the signals of the dendrimer (l). Using any of the remaining non-overlapping signals, an estimate of the number of SA molecules successfully conjugated onto the dendrimer could be made. It was found that an average of 33 and 60 SA molecules were conjugated to G4.NH$_2$ and G5.NH$_2$, respectively. Since the G4.NH$_2$ PAMAM dendrimer has a total of 64 surface groups and G5.NH$_2$ has 128 surface groups, it is possible to conclude that ~50% surface functionalization was achieved in each case. Additionally, further analysis of the SAGx ^{1}H NMR spectra (Figs. 24D and 25D) demonstrated a slight shift in the signals of SA and Gx after functionalisation, with signal f being the most noticeable. Since proton type f is the closest to the group that binds to the dendrimer, it makes sense that this is the signal that shows the highest shift from its original position after conjugation. Furthermore, the absence of signals in their original positions for SA in the SAGx spectra indicates that there is no unbound SA, which in turn reveals that any excess SA or by-products were effectively removed during dialysis.

In the case of the Cu-containing SAGx samples, NMR analysis was only used to determine the presence of Cu through possible shifts and to detect the presence of contaminants such as AA that may not have been completely removed during the purification step. From the spectra shown in Figs. 24E and 25E, it is clear that the CuSAGx samples exhibit the same signals present in the SAGx complexes, with the signals showing a slight shift that may be related to the presence of either AA or Cu. Moreover, the CuSAGx samples show the appearance of three new signals g, h and i, which as demonstrated by UV-Vis analysis (section 3.2.1) strongly indicate the presence of AA in the samples. Regardless, there is a difference in one of the signals referring to AA. More specifically, signal i has significantly shifted from its initial position at

4.959 ppm to 4.511 ppm. Since AA is highly unstable, especially at high temperatures for long periods of time, this phenomenon may pertain to its degradation into 2,3-diketogluconic acid (DKG).[178,179] It is worth mentioning that, as expected, the purification extract (i.e., CuSAGx imp) also contained DKG (see Figs. 24F and 25F), which consolidates the idea that the different CuSAGx samples were not completely purified. It is important to note that due to the low signal resolution in the spectra obtained for the CuSAGx samples, it was impossible to integrate the signals and get an in-depth analysis.
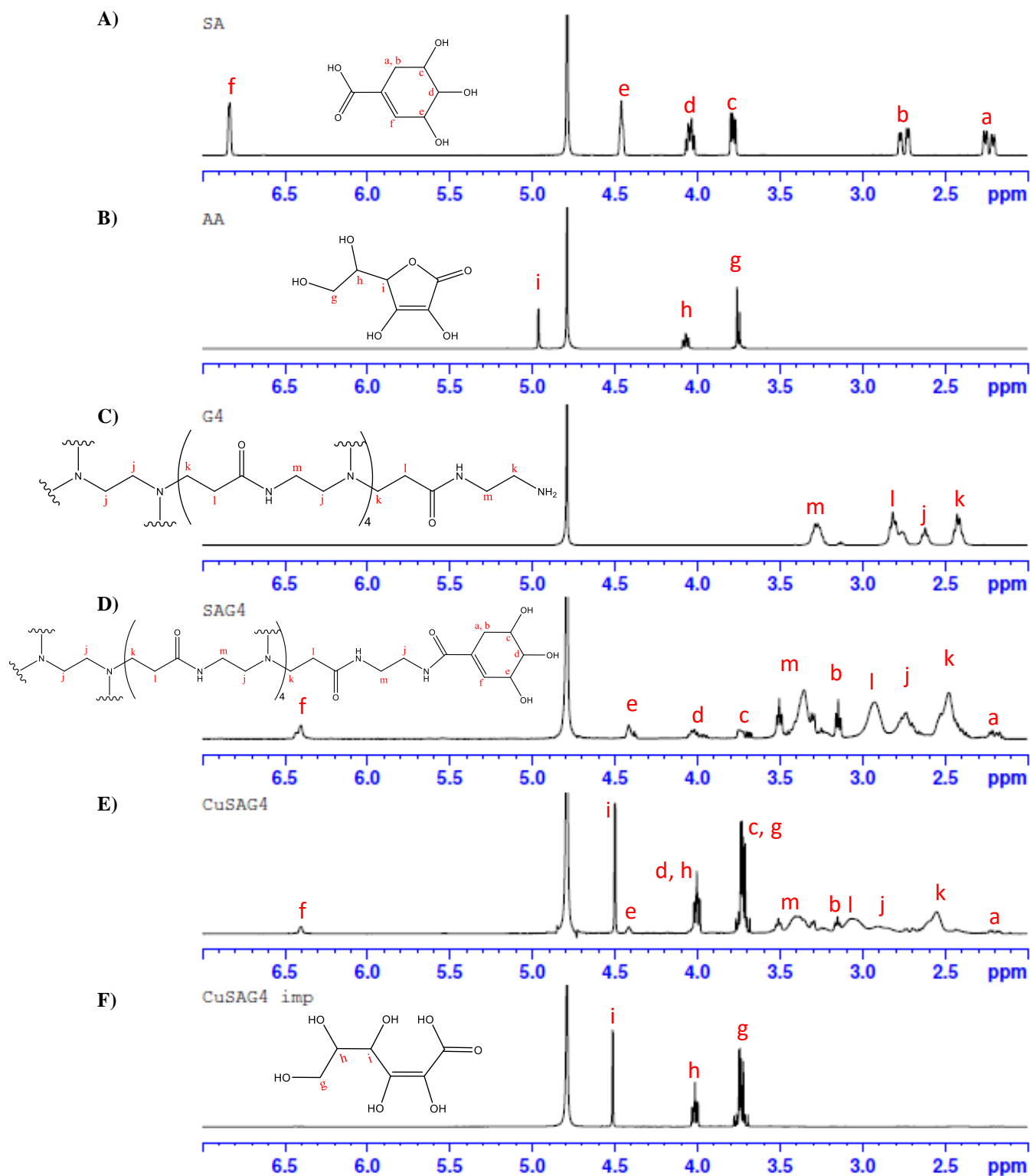
Figure 24 – ^{1}H NMR spectra of (A) SA, (B) AA, (C) G4.NH$_2$ PAMAM, (D) SAG4, (E) CuSAG4 and (F) CuSAG4/imp. The chemical structures of SA, AA, G4.NH$_2$ PAMAM and SAG4 are indicated in each respective spectrum and the corresponding signal/structure identification. (400 MHz, D$_2$O, δ = 4.790 ppm).
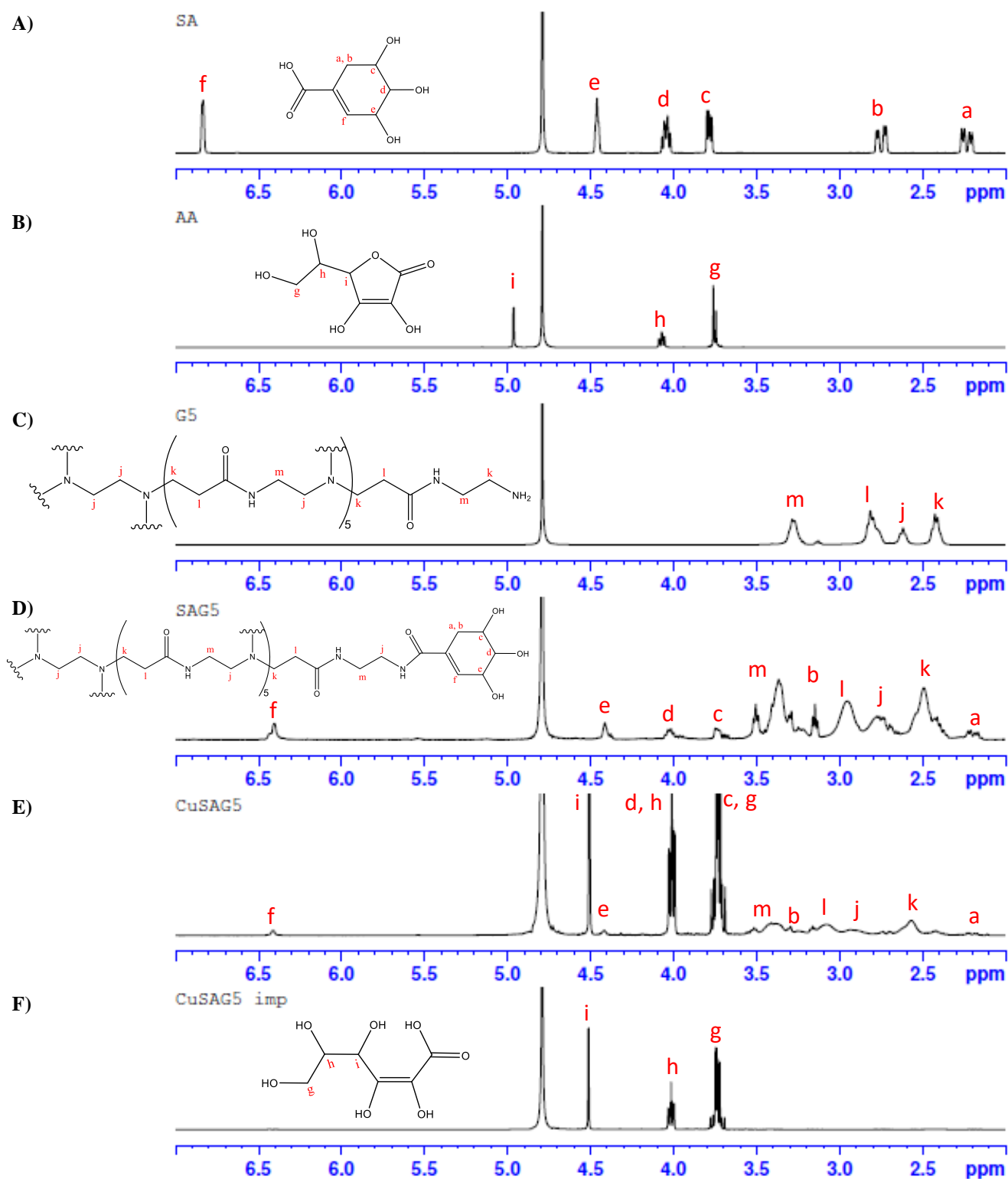
Figure 25 – ^{1}H NMR spectra of (A) SA, (B) AA, (C) G5.NH₂ PAMAM, (D) SAG5, (E) CuSAG5 and (F) CuSAG5/imp. The chemical structures of SA, AA, G5.NH₂ PAMAM and SAG5 are indicated in each respective spectrum and the corresponding signal/structure identification. (400 MHz, D₂O, δ = 4.790 ppm)

3.2.5. DLS analysis

To assess the hydrodynamic size of the prepared SAGx and CuSAGx samples, DLS studies were performed (see Table 3). The experimental data obtained for the G4.NH$_2$ PAMAM dendrimer was 5.4 nm while G5.NH$_2$ PAMAM dendrimer size was 7.6 nm, which is in accordance with the data reported by the manufacturer (4.5 and 5.4 nm, respectively).[171] Comparing the data obtained for each unmodified dendrimer with that obtained from the respective SAGx complexes, an increase in the hydrodynamic radius was evident, which can serve as an extra indicator of the success of the coupling reaction. On the other hand, the CuSAGx samples experienced a decrease in the hydrodynamic radius relative to the respective SAGx conjugates. This phenomenon may be linked to the presence of Cu in the sample and the interactions it establishes with the dendrimer, causing its branches to collapse over each other.[171] However more studies would need to be performed to confirm this.

Table 3 – Size of the SA-functionalised PAMAM dendrimers (SAGx) and the respective Cu DENPs. The data for the SA, G4 and G5 starting reagents is also shown. All samples were prepared in ultrapure water at a concentration of 0.5 mg/ml.

Compound	**Size (nm)**	**PDI**
G4.NH$_2$	5.4 ± 0.1	0.30 ± 0.01
G5.NH$_2$	7.6 ± 0.4	0.34 ± 0.14
SAG4	19.1 ± 1.1	0.83 ± 0.04
SAG5	18.8 ± 1.5	0.87 ± 0.07
CuSAG4	9.1 ± 0.4	0.24 ± 0.01
CuSAG5	13.1 ± 0.2	0.25 ± 0.04

Typically, samples with polydispersity index (PDI) values below 0.1 are considered highly monodisperse, while values between 0.1 and 0.4 are deemed moderately polydisperse. Anything above that threshold is deemed highly polydisperse.[158] According to this information, and based on the PDI values reported in Table 3, all the samples may be considered moderately or highly polydisperse. With a PDI of approximately 0.8, the SAGx conjugates may be

considered as the most polydisperse. Contrastingly, each dendrimer and the respective CuSAGx complexes have PDI values in the range of ~0.2 and 0.3 and may be considered as moderately polydisperse.

3.2.6.   SEM coupled with EDX spectroscopy analysis

To observe the morphology of the CuSAGx samples and quantify the presence of Cu in each one, the samples were submitted to SEM/EDX analysis. From Fig. 26, it is readily visible that in the images of both CuSAG4 and the CuSAG5, there is the predominance of a dark background with some lighter spots randomly distributed throughout the field of view. In SEM the presence of this dark background colour is originated by the organic component of the sample (i.e., the dendrimer) and the lighter spots are related to the existence of heavier elements such as metals.

After freeze-dried, the CuSAGx samples had a crystal-like powder appearance. However, since sample preparation was carried out on a different day than the SEM analysis, each CuSAGx sample changed in appearance while in the holder. The change from an initially crystal-like powder to a smoother appearance as can be seen in the images in Fig. 26 may be a result of the samples absorbing moisture from the atmosphere.
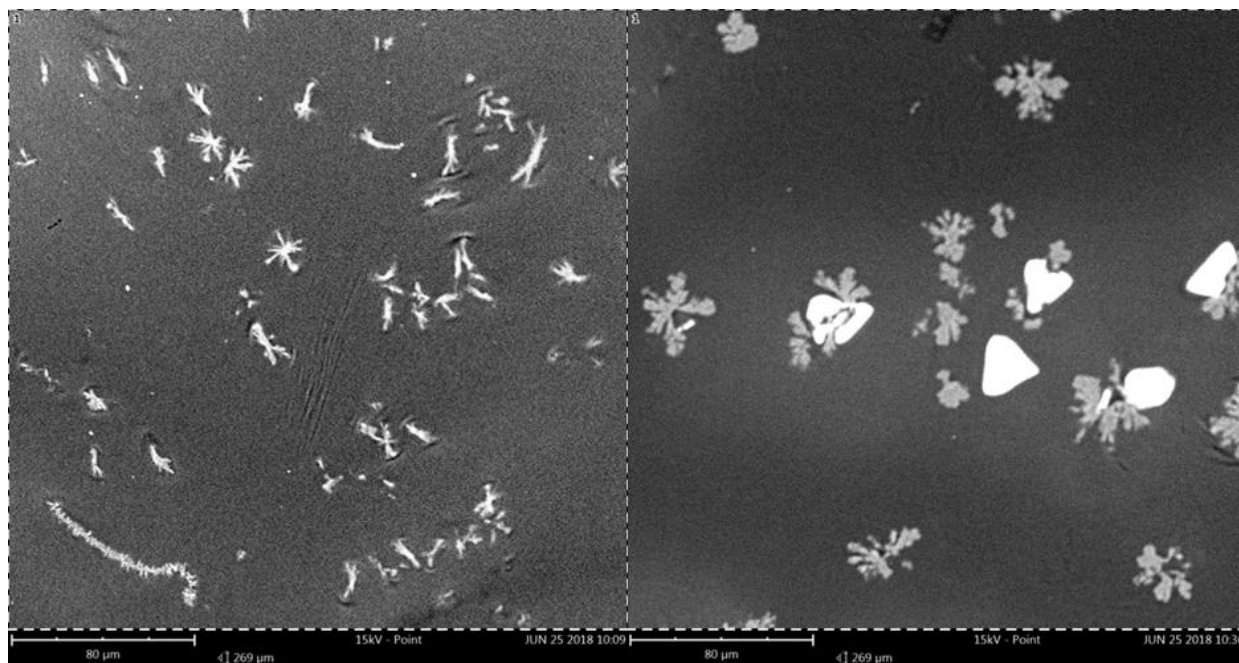
Figure 26 – SEM images of the CuSAG4 (left) and the CuSAG5 (right) samples.

EDX analysis of each area represented in Fig. 26 showed that the CuSAG4 sample had 69.05% of oxygen, 12.83% of carbon, 11.08% of sodium, 4.87% of nitrogen and 2.17% of chlorine, while the CuSAG5 sample had 70.89% of oxygen, 17.01% of sodium, 8.01% of carbon, 1.95% of nitrogen, and 2.13% of chlorine. However, no Cu was detected in the matrix in each case, or at least not enough for it to be detected by the technique. These results lead to the conclusion that the structures represented in Fig. 26 are likely attributable to the synthesis process, where sodium hydroxide and hydrochloric acid were used to regulate the pH of the reaction mix. The lack of Cu in the organic matrix is most likely explained by the deposit obtained at the bottom of the flask after the reaction (refer to section 3.1).

3.2.7. ICP–OES analysis

The ICP-OES analysis of the CuSAGx samples are reported in Table 4. When comparing the 0.083% and 0.012% Cu content in CuSAG4 and CuSAG5, respectively, it is evident that the Cu content in the first is greater than in the latter. Moreover, the Cu content of each sample was less than 1%, which is in accordance with the results obtained by SEM analysis (section 3.2.2). These results once again indicate that the lack of Cu in each sample may likely be explained by the deposit in the round-bottomed flask after the reaction (refer to section 3.1).

Table 4 – Percentage of Cu in the CuSAG4 and CuSAG5 compounds.

Compound	**%Cu**
CuSAG4	0.083
CuSAG5	0.012

3.3. Cytotoxicity

The effect of the prepared SA-functionalized PAMAM dendrimers and the respective Cu DENPs on cell viability was assessed using the resazurin assay. For this, HEK 293T cells were exposed to increasing concentrations of each SAGx sample, as well as SA and the unmodified PAMAM dendrimers under investigation.

From Fig. 27, analysis led to the conclusion that the tendency was for cell viability to decrease as the concentration of the compound under investigation increased. Comparing the two generations of dendrimer used, the G4.NH$_2$ PAMAM dendrimer presented lower cytotoxicity (e.g., 74% cell viability when using 10 μM) relative to the G5.NH$_2$ PAMAM dendrimer (e.g., 7% cell viability when using 10 μM). These results follow what is found in the literature, proving that as reported, cell viability is inversely proportional to the surface amine content in PAMAM dendrimers.[180] In the case of the cells exposed to 1 mM SA, it is clear that alone it does not cause harm and may be considered as biocompatible. For the SA-functionalised PAMAM dendrimers, on the other hand, the data showed that overall cytotoxicity increased

with increasing sample concentration. Regardless, unlike the SAG5 conjugate, which even at the maximum concentration tested still presented nearly 80% cell viability, the SAG4 conjugate caused a steep decrease in cell viability at 400 µM with only 5% of viable cells. Taken as a whole, these results lead to the conclusion that, as previously reported, surface modification of cationic PAMAM dendrimers may indeed attenuate their cytotoxicity.[180] Moreover, the SA-functionalised PAMAM dendrimers prepared in this study may be considered as biocompatible. However, despite these positive results, it is important to note that to obtain results closer to reality, the prepared SA-functionalised PAMAM dendrimers should also be tested on DCs in general, but especially in LCs.
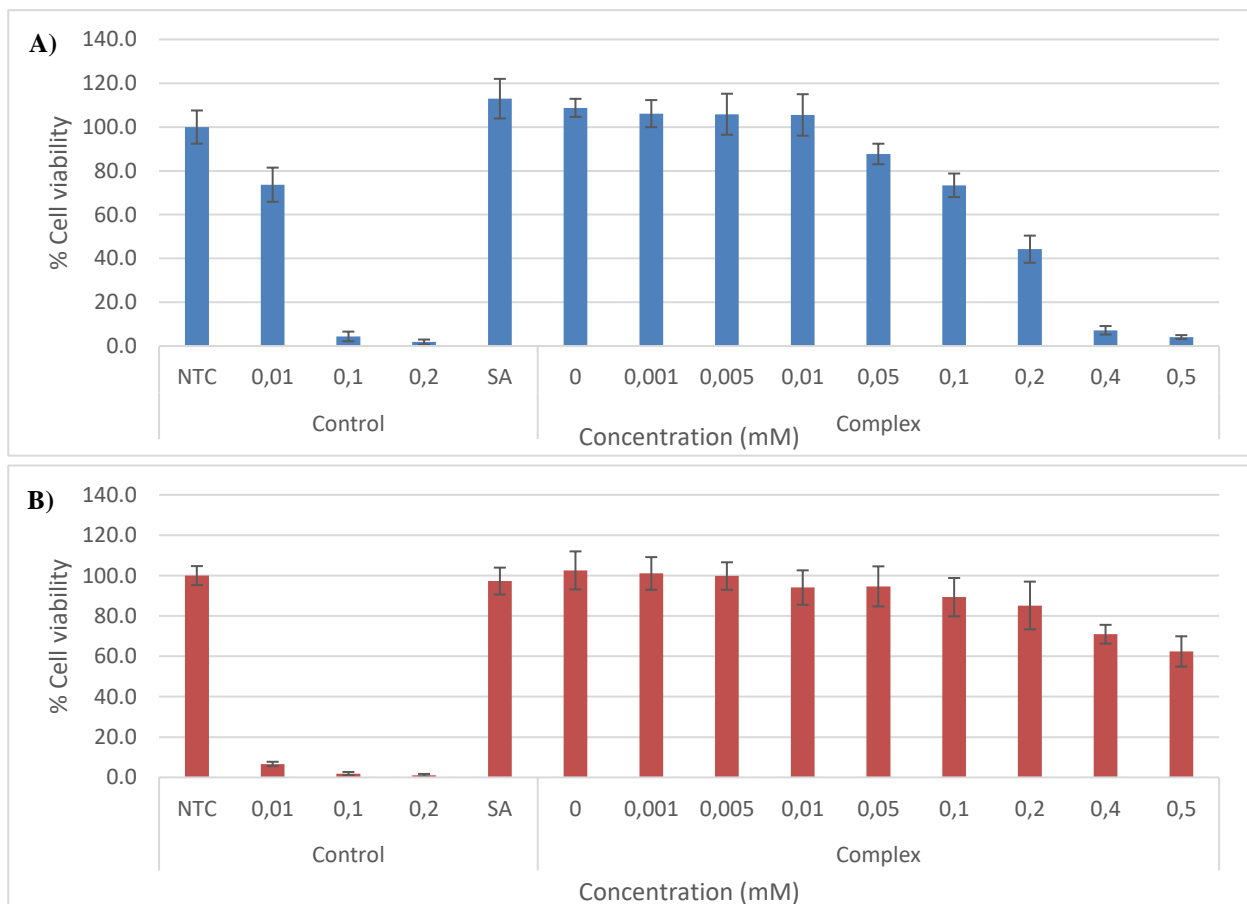
Figure 27 – Cell viability of HEK 293T cells when exposed to (A) 0.01, 0.1 and 0.2 mM of the G4.NH$_2$ PAMAM dendrimer, 1 mM SA and 0, 0.001, 0.005, 0.01, 0.05, 0.1, 0.2, 0.4 and 0.5 mM of the SA-functionalized G4.NH$_2$ PAMAM dendrimer and (B) 0.01, 0.1 and 0.2 mM of the G5.NH$_2$ PAMAM dendrimer, 1 mM SA and 0, 0.001, 0.005, 0.01, 0.05, 0.1, 0.2, 0.4 and 0.5 mM of the SA-functionalized G5.NH$_2$ PAMAM dendrimer.

4.   CONCLUSIONS

With the aim of inhibiting the entry of DENV and ZIKV into host DCs, a novel glycodendrimer-based system was prepared in this study. Combining the inherent biocompatibility of SA and the multivalency and versatility of the dendrimers, G4.NH$_2$ and G5.NH$_2$ PAMAM dendrimers were used as scaffolds to successfully conjugate SA to their surface via EDC/NHS coupling chemistry.[111] Due to the know antiviral properties of Cu[127,128], the prepared SA-functionalised dendrimers were then used in an attempt to prepare Cu DENPs with the intent of also neutralising the viral particles, however, this milestone was not accomplished.

Overall, the attachment of SA onto PAMAM dendrimer scaffold proved to be a rather easy step, which rendered approximately 50% of functionalisation in both generations used. Of all the techniques used to characterise the SAGx compounds, the one that provided the most valuable structural information was ^{1}H NMR spectroscopy, since not only did it confirm the conjugation had been successful, but also, gave an idea of the degree of functionalisation of the dendrimer. In the case of ATR-FTIR, complementary structural data was acquired for all the prepared samples. In the DLS studies, the data clearly showed that after the coupling reaction to produce the SA-functionalised dendrimers, the hydrodynamic radius of each PAMAM dendrimer increased, which can serve as an indication of the success of the reaction.

Combining all the information gathered by the different characterisation techniques, mainly UV-Vis, EDX and ICP-OES, it was possible to conclude that Cu NPs were not successfully entrapped in the SAGx systems. In order to obtain and stabilise the Cu NPs in the developed systems, the synthetic process would need to be altered either by changing the reducing agent, changing the reaction times or even changing other experimental conditions (e.g., pH of the reaction mixture, or using a biocompatible buffer). Contrary to what happened in the first step of the synthesis when preparing the SA-functionalised dendrimers, the hydrodynamic radius of the CuSAGx samples decreased, which may have been caused by the presence of Cu. To stabilise and improve the obtention of Cu NPs, perhaps an alternative to AA would be the use of plant extracts, which is also known as green chemistry.

Ultimately, one of the final objectives of this work would be to create a system that can effectively target the DC-SIGN receptor. As a complement to the experimental data acquired in

this work, molecular dynamics simulation studies would be interesting to implement in order to acquire more information on how the prepared SAGx and CuSAGx samples interact with the target receptor. After this, the next phase of the work would consist of studies focused on the analysis of interactions of each sample with the DC-SIGN receptor either against transfected cells or actual DCs.

In brief, this study opens the door to exploring the use of the developed SA-functionalised PAMAM dendrimers and their Cu DENP counterparts as novel DC-SIGN antagonists targeting infectious diseases such as dengue and zika. Furthermore, due to the similarities across the Flaviviridae family, this may be a valuable asset not only against the previously mentioned diseases, but also against other viruses of the same family.

5.   FUTURE PERSPECTIVES

Due to the natural difficulties that come with scientific research and have led to lack of time for more exploration, there is still room for improvement, especially when it comes to biocompatibility and binding affinity assessment. As such, besides exploring new ideas to effectively entrap Cu NPs in the dendrimer scaffold and maybe trying to encapsulate different metals with antiviral activity, it is also extremely necessary to test the stability of the prepared SAGx and CuSAGx complexes under different temperature and pH conditions to ensure its use in biomedical applications. Furthermore, to assess the effectiveness of the conjugates, binding-affinity studies where the interaction between the two different SA-functionalised PAMAM dendrimers and their Cu DENP counterparts with DC-SIGN are also needed. Additionally, cytotoxicity studies in DCs are of the utmost importance to assess the effect of all the prepared complexes on the target cells, and potentially establish their mechanism of action *in vitro*. Finally, depending on the biocompatibility of the prepared complexes, studies focused on antiviral activity testing would be the next step to provide insights into how the developed systems compare with pre-existing antiviral drugs.

6.   REFERENCES

(1)   Cruz-Oliveira, C.; Freire, J. M.; Conceição, T. M.; Higa, L. M.; Castanho, M. A. R. B.; Da Poian, A. T. Receptors and Routes of Dengue Virus Entry into the Host Cells. *FEMS Microbiol. Rev.* **2015**, *39* (2), 155–170. https://doi.org/10.1093/femsre/fuu004.

(2)   Garber, K. C. A.; Wangkanont, K.; Carlson, E. E.; Kiessling, L. L. A General Glycomimetic Strategy Yields Non-Carbohydrate Inhibitors of DC-SIGN. *R. Soc. Chem.* **2010**, *46* (36), 6747–6749. https://doi.org/10.1039/c0cc00830c.

(3)   Henchal, E. A.; Putnak, J. R. The Dengue Viruses. *Clin. Microbiol. Rev.* **1990**, *3* (4), 376–396. https://doi.org/10.1128/CMR.3.4.376.

(4)   Saeed, M. A.; Attia, T. H. Dengue and Dengue Hemorrhagic Fever. *Afro-Egypt J Infect Endem Dis* **2015**, *5* (3), 189–200.

(5)   Raheel, U.; Faheem, M.; Riaz, M. N.; Kanwal, N.; Javed, F. Regional Review Dengue Fever in the Indian Subcontinent: An Overview. *J. Infect. Dev. Ctries.* **2011**, *5* (4), 239–247. https://doi.org/10.3855/jidc.1017.

(6)   Dick, O. B.; San Martín, J. L.; Montoya, R. H.; Del Diego, J.; Zambrano, B.; Dayan, G. H. Review: The History of Dengue Outbreaks in the Americas. *Am. Soc. Trop. Med. Hyg.* **2012**, *87* (4), 584–593. https://doi.org/10.4269/ajtmh.2012.11-0770.

(7)   World Health Organization. Zika virus www.who.int/news-room/fact-sheets/detail/zika-virus (accessed Sep 24, 2018).

(8)   Rocha, D.; Olivia, M.; Maria, T.; Ana, C.; Manuel, D.; Chtistina, M. Larvicidal Activity against Aedes Aegypti of Foeniculum Vulgare Essential Oils from Portugal and Cape Verde. *Nat. Prod. Commun.* **2015**, *10* (4), 677–682. https://doi.org/10.1073/pnas.0703993104.

(9)   World Health Organization. Emergencies - The history of Zika virus http://www.who.int/emergencies/zika-virus/timeline/en/ (accessed Oct 10, 2020).

(10)   Pan American Health Organization. CASES OF ZIKA VIRUS https://www.paho.org/data/index.php/en/?option=com_content&view=article&id=524:z

ika-weekly-en&Itemid=352 (accessed Oct 25, 2019).

(11) Paixão, E. S.; Teixeira, M. G.; Rodrigues, L. C. Zika, Chikungunya and Dengue: The Causes and Threats of New and Re-Emerging Arboviral Diseases. *BMJ Glob. Heal.* **2017**, *3*, 1–6. https://doi.org/10.1136/bmjgh-2017-000530.

(12) Beltrán-Silva, S. L.; Chacón-Hernández, S. S.; Moreno-Palacios, E.; Pereyra-Molina, J. Á. Clinical and Differential Diagnosis: Dengue, Chikungunya and Zika. *Rev. Médica del Hosp. Gen. México* **2018**, *81* (3), 146–153. https://doi.org/10.1016/j.hgmx.2016.09.011.

(13) Gubler, D. J. Dengue and Dengue Hemorrhagic Fever. *Clin. Microbiol. Rev.* **1998**, *11* (3), 480–496. https://doi.org/10.1128/CMR.11.3.480.

(14) World Health Organization. Dengue and severe dengue Key facts Global burden of dengue Distribution and outbreaks of dengue Disease characteristics (signs and symptoms) Vaccination against dengue https://www.who.int/news-room/fact-sheets/detail/dengue-and-severe-dengue.

(15) Musso, D.; Roche, C.; Robin, E.; Nhan, T.; Teissier, A.; Cao-Lormeau, V. M. Potential Sexual Transmission of Zika Virus. *Emerg. Infect. Dis.* **2015**, *21* (2), 359–361. https://doi.org/10.3201/eid2102.141363.

(16) Petersen, L. R.; Jamieson, D. J.; Powers, A. M.; Honein, M. A. Zika Virus (Review Article). *N. Engl. J. Med.* **2016**, *374* (16), 1552–1563. https://doi.org/10.1056/NEJMra1602113.

(17) Sutiono, D. R.; Gunawan, J. D. Dengue, Chikungunya, and Zika: Differences in Similarities. *Indones. Int. Inst. Life Sci.* **2017**, *44* (3), 176–178.

(18) Carteaux, G.; Maquart, M.; Bedet, A.; et Al. Zika Virus Associated with Meningoencephalitis. *N. Engl. J. Med.* **2016**, No. Panel C, 1–3. https://doi.org/10.1056/NEJMc1603618.

(19) Mécharles, S.; Herrmann, C.; Poullain, P.; Tran, T.-H.; Deschamps, N.; Mathon, G.; Landais, A.; Breurec, S.; Lannuzel, A. Acute Myelitis Due to Zika Virus Infection. *Lancet* **2016**, *387* (10026), 1481. https://doi.org/10.1016/S0140-6736(16)00644-9.

(20) Foy, B. D.; Kobylinski, K. C.; Foy, J. L. C.; Blitvich, B. J.; da Rosa, A. T.; Haddow, A. D.; Lanciotti, R. S.; Tesh, R. B. Probable Non-Vector-Borne Transmission of Zika Virus,

Colorado, USA. *Emerg. Infect. Dis.* **2011**, *17* (5), 880–882. https://doi.org/10.3201/eid1705.101939.

(21)   Arun Asif, Sobia Manzoor, Fatima-Tuz-Zahra, Muhammad Saalim, Maliha Ashraf, Javeria Ishtiyaq, and M. K. Zika Virus: A Review of Literature. *Viruses* **2018**, *9* (12), 1–5. https://doi.org/10.7759/cureus.3025.

(22)   Centers for Disease Control and Prevention. Microcephaly & Other Birth Defects https://www.cdc.gov/zika/healtheffects/birth_defects.html.

(23)   Dieng, H.; Saifur, R. G. M.; Ahmad, A. H.; Che Salmah, M. R.; Aziz, A. T.; Satho, T.; Miake, F.; Jaal, Z.; Abubakar, S.; Morales, R. E. Unusual Developing Sites of Dengue Vectors and Potential Epidemiological Implications. *Asian Pac. J. Trop. Biomed.* **2012**, *2* (3), 228–232. https://doi.org/10.1016/S2221-1691(12)60047-1.

(24)   Clemons, A.; Haugen, M.; Flannery, E.; Tomchaney, M.; Kast, K.; Jacowski, C.; Le, C.; Mori, A.; Holland, W. S.; Sarro, J.; Severson, D. W.; Duman-Scheel, M. Aedes Aegypti: An Emerging Model for Vector Mosquito Development. *Cold Spring Harb. Protoc.* **2010**, *5* (10). https://doi.org/10.1101/pdb.emo141.

(25)   Kamal, M.; Kenawy, M. A.; Rady, M. H.; Khaled, A. S.; Samy, A. M. Mapping the Global Potential Distributions of Two Arboviral Vectors Aedes Aegypti and Ae. Albopictus under Changing Climate. *PLoS One* **2018**, *13* (12), 1–21. https://doi.org/10.1371/journal.pone.0210122.

(26)   Weeratunga, P.; Rodrigo, C.; Fernando, S. D.; Rajapakse, S. Control Methods for Aedes Albopictus and Aedes Aegypti. *Cochrane Database Syst. Rev.* **2017**, *2017* (8). https://doi.org/10.1002/14651858.CD012759.

(27)   Biogents. Life Cycle of Aedes Mosquitoes - Eco-Friendly Mosquitotraps https://sea.biogents.com/life-cycle-aedes-mosquitoes/ (accessed Oct 21, 2019).

(28)   van den Berg, H.; Zaim, M.; Yadav, R. S.; Soares, A.; Ameneshewa, B.; Mnzava, A.; Hii, J.; Dash, A. P.; Ejov, M. Global Trends in the Use of Insecticides to Control Vector-Borne Diseases. *Environ. Health Perspect.* **2012**, *120* (4), 577–582. https://doi.org/10.1289/ehp.1104340.

(29)   Gubler, D. J.; Clark, G. G. Community Involvement in the Control of Aedes Aegypti.

Acta Trop. **1996**, *61* (2), 169–179. https://doi.org/10.1016/0001-706X(95)00103-L.

(30)   Hurst, T. P.; Pittman, G.; O'Neill, S. L.; Ryan, P. A.; Le Nguyen, H.; Kay, B. H. Impacts of Wolbachia Infection on Predator Prey Relationships: Evaluating Survival and Horizontal Transfer Between w MelPop Infected Aedes Aegypti and Its Predators: Table 1. *J. Med. Entomol.* **2012**, *49* (3), 624–630. https://doi.org/10.1603/me11277.

(31)   Seng, C. M.; Setha, T.; Nealon, J.; Socheat, D.; Chantha, N.; Nathan, M. B. Community-Based Use of the Larvivorous Fish Poecilia Reticulata to Control the Dengue Vector Aedes Aegypti in Domestic Water Storage Containers in Rural Cambodia. *J. Vector Ecol.* **2008**, *33* (1), 139–144. https://doi.org/10.3376/1081-1710(2008)33[139:cuotlf]2.0.co;2.

(32)   Alphey, L.; McKemey, A.; Nimmo, D.; Neira Oviedo, M.; Lacroix, R.; Matzen, K.; Beech, C. Genetic Control of Aedes Mosquitoes. *Pathog. Glob. Health* **2013**, *107* (4), 170–179. https://doi.org/10.1179/2047773213Y.0000000095.

(33)   Centers for Disease Control and Prevention. Integrated Mosquito Management | Zika virus | CDC https://www.cdc.gov/zika/vector/integrated_mosquito_management.html.

(34)   Centers for Disease Control and Prevention. Controlling Mosquitoes at Home | Zika Virus | CDC https://www.cdc.gov/zika/prevention/controlling-mosquitoes-at-home.html%0AControlling (accessed Oct 21, 2019).

(35)   World Health Organization. Dengue Vaccines.

(36)   Vidyasagar, A. What Are Viruses? https://www.livescience.com/53272-what-is-a-virus.html%0AViruses (accessed Jan 11, 2020). https://doi.org/10.1017/CBO9781107415324.004.

(37)   Ferreira, W. F. C.; Sousa, J. C. F. de; Lima, N. *Microbiologia - Cap. 6: Virus*; LIDEL - Edições Técnicas, Ldª: Lisboa, 2010.

(38)   Thomas J. Chambers; Monath, T. P.; Maramorosch, K.; Shatkin, A. J.; Murphy, F. A. *THE FLAVIVIRUSES: STRUCTURE, REPLICATION AND EVOLUTION*, 1st ed.; Press, E. A., Ed.; Academic Press, 2003; Vol. 59.

(39)   Knipe, D. M.; Howley, P. M. *Fields Virology*, 6th ed.; Wilkins, L. W. &, Ed.; LWW, 2013; Vol. 1 & 2. https://doi.org/10.1016/S0168-7069(08)70099-5.

(40)   International Committee on Taxonomy of Viruses. Genus: Flavivirus - Flaviviridae -

Positive-sense RNA Viruses.

(41) *Virus Taxonomy: Classification and Nomenclature of Viruses*; 1995. https://doi.org/10.1016/b978-0-12-384684-6.00012-4.

(42) King, A. M.; Lefkowitz, E.; Adams, M. J.; Carstens, E. B. *Virus Taxonomy: Classification and Nomenclature of Viruses*, 1st ed.; Andrew M.Q. King, Michael J. Adams, Eric B. Carstens, and and E. J. L., Ed.; Elsevier, 2011.

(43) Brown, E.; Bentham, M.; Beaumont, H.; Bloy, A.; Thompson, R.; McKimmie, C.; Foster, R.; Ranson, N.; Maconald, A.; Kalli, A.; Griffin, S. Flavivirus Membrane (M) Proteins as Potential Ion Channel Antiviral Targets (VERIFICAR). *J. Chem. Inf. Model.* **2013**, *53* (9), 1689–1699. https://doi.org/10.1017/CBO9781107415324.004.

(44) Lindenbach, B. D.; Thiel, H.-J.; Rice, C. M. Flaviviridae: The Viruses and Their Replication. In *Fields Virology*; Minarno, Eko Budi and Hariani, L., Ed.; Philadelphia, 2008; pp 1101–1152. https://doi.org/10.1016/0038-092X(88)90131-4.

(45) Nature Education. Dengue Viruses https://www.nature.com/scitable/topicpage/dengue-viruses-22400925/ (accessed Jan 1, 2019). https://doi.org/10.1016/S0140-6736(80)92916-5.

(46) Chang, H.-H.; Huber, R. G.; Bond, P. J.; Grad, Y. H.; Camerini, D.; Maurer-Stroh, S.; Lipsitch, M. Systematic Analysis of Protein Identity between Zika Virus and Other Arthropod-Borne Viruses. *Bull. World Health Organ.* **2017**, *95* (7), 517-525I. https://doi.org/10.2471/blt.16.182105.

(47) Beck, C.; Jimenez-Clavero, M. A.; Leblond, A.; Durand, B.; Nowotny, N.; Leparc-Goffart, I.; Zientara, S.; Jourdain, E.; Lecollinet, S. Flaviviruses in Europe: Complex Circulation Patterns and Their Consequences for the Diagnosis and Control of West Nile Disease. *Int. J. Environ. Res. Public Health* **2013**, *10* (11), 6049–6083. https://doi.org/10.3390/ijerph10116049.

(48) Zhang, X.; Jia, R.; Shen, H.; Wang, M.; Yin, Z.; Cheng, A. Structures and Functions of the Envelope Glycoprotein in Flavivirus Infections. *Viruses* **2017**, *9* (11), 1–14. https://doi.org/10.3390/v9110338.

(49) Yap, S. S. L.; Nguyen-Khuong, T.; Rudd, P. M.; Alonso, S. Dengue Virus Glycosylation:

What Do We Know? *Front. Microbiol.* **2017**, *8* (JUL), 1–16. https://doi.org/10.3389/fmicb.2017.01415.

(50) Wen, D.; Li, S.; Dong, F.; Zhang, Y.; Lin, Y.; Wang, J.; Zou, Z.; Zheng, A. N-Glycosylation of Viral e Protein Is the Determinant for Vector Midgut Invasion by Flaviviruses. *MBio* **2018**, *9* (1), 1–14. https://doi.org/10.1128/mBio.00046-18.

(51) Carbaugh, D. L.; Baric, R. S.; Lazear, H. M. Envelope Protein Glycosylation Mediates Zika Virus Pathogenesis. *J. Virol.* **2019**, *93* (12), 1–16. https://doi.org/10.1128/jvi.00113-19.

(52) Alberts, B.; Johnson, A.; Lewis, J.; Raff, M.; Roberts, K.; Walter, P. *Molecular Biology of the Cell*, 5th ed.; Granum, M. A. and S., Ed.; Garland Science: New York, UK, 2008.

(53) Sironi, M.; Forni, D.; Clerici, M.; Cagliani, R. Nonstructural Proteins Are Preferential Positive Selection Targets in Zika Virus and Related Flaviviruses. *PLoS Negl. Trop. Dis.* **2016**, *10* (9), 1–18. https://doi.org/10.1371/journal.pntd.0004978.

(54) Palucka, A. K. Dengue Virus and Dendritic Cells. *Nat. Med.* **2000**, *6* (7), 748–749. https://doi.org/10.1038/77470.

(55) Nature Education. Host Response to the Dengue Virus http://www.nature.com/scitable/topicpage/host-response-to-the-dengue-virus-22402106.

(56) Rey, F. A. Dengue Virus Envelope Glycoprotein Structure: New Insight into Its Interactions during Viral Entry. *Proc. Natl. Acad. Sci. U. S. A.* **2003**, *100* (12), 6899–6901. https://doi.org/10.1073/pnas.1332695100.

(57) Rice University. 21.1 Anatomy of the Lymphatic and Immune Systems - Anatomy and Physiology https://opentextbc.ca/anatomyandphysiology/chapter/21-1-anatomy-of-the-lymphatic-and-immune- systems/%0A138 (accessed Oct 9, 2018).

(58) Collin, M.; Mcgovern, N.; Haniffa, M. Human Dendritic Cell Subsets. *Immunology* **2013**, *140* (1), 22–30. https://doi.org/10.1111/imm.12117.

(59) de Jong, M. A. W. P.; Vriend, L. E. M.; Theelen, B.; Taylor, M. E.; Fluitsma, D.; Boekhout, T.; Geijtenbeek, T. B. H. C-Type Lectin Langerin Is a β-Glucan Receptor on Human Langerhans Cells That Recognizes Opportunistic and Pathogenic Fungi. *Mol. Immunol.* **2010**, *47* (6), 1216–1225. https://doi.org/10.1016/j.molimm.2009.12.016.

(60) Elong Ngono, A.; Shresta, S. Immune Response to Dengue and Zika. *Annu. Rev. Immunol.* **2018**, *36* (1), 279–308. https://doi.org/10.1146/annurev-immunol-042617-053142.

(61) Perera-Lecoin, M.; Meertens, L.; Carnec, X.; Amara, A. Flavivirus Entry Receptors: An Update. *Viruses* **2014**, *6* (1), 69–88. https://doi.org/10.3390/v6010069.

(62) Taylor, A.; Foo, S. S.; Bruzzone, R.; Vu Dinh, L.; King, N. J. C.; Mahalingam, S. Fc Receptors in Antibody-Dependent Enhancement of Viral Infections. *Immunol. Rev.* **2015**, *268* (1), 340–364. https://doi.org/10.1111/imr.12367.

(63) Khandia, R.; Munjal, A.; Dhama, K.; Karthik, K.; Tiwari, R.; Malik, Y. S.; Singh, R. K.; Chaicumpa, W. Modulation of Dengue/Zika Virus Pathogenicity by Antibody-Dependent Enhancement and Strategies to Protect against Enhancement in Zika Virus Infection. *Front. Immunol.* **2018**, *9* (597), 1–17. https://doi.org/10.3389/fimmu.2018.00597.

(64) Klimstra, W. B.; Nangle, E. M.; Smith, M. S.; Yurochko, A. D.; Ryman, K. D. DC-SIGN and L-SIGN Can Act as Attachment Receptors for Alphaviruses and Distinguish Between Mosquito Cell-and Mammalian Cell-Derived Viruses. *J. Virol.* **2003**, *77* (22), 12022–12032. https://doi.org/10.1128/JVI.77.22.12022–12032.2003.

(65) Perera, R.; Khaliq, M.; Kuhn, R. J. Closing the Door on Flaviviruses: Entry as a Target for Antiviral Drug Design. *Antiviral Res.* **2008**, *80* (1), 11–22. https://doi.org/10.1016/j.antiviral.2008.05.004.

(66) Sirohi, D.; Kuhn, R. J. Zika Virus Structure, Maturation, and Receptors. *J. Infect. Dis.* **2017**, *216* (Suppl 10), S935–S944. https://doi.org/10.1093/infdis/jix515.

(67) Ye, J.; Zhu, B.; Fu, Z. F.; Chen, H.; Cao, S. Immune Evasion Strategies of Flaviviruses. *Vaccine* **2013**, *31* (3), 461–471. https://doi.org/10.1016/j.vaccine.2012.11.015.

(68) Byk, L. A.; Gamarnik, A. V. Properties and Functions of the Dengue Virus Capsid Protein. *Annu. Rev. Virol.* **2016**, *3* (1), 263–281. https://doi.org/10.1146/annurev-virology-110615-042334. Properties.

(69) Screaton, G.; Mongkolsapaya, J.; Yacoub, S.; Roberts, C. New Insights Into the Immunopathology and Control of Dengue Virus Infection. *Nat. Rev. Immunol.* **2015**, *15* (12), 745–759. https://doi.org/10.1038/nri3916.

(70) Diseases, N. I. of A. and I. Ted Pierson, Ph.D. | NIH: National Institute of Allergy and Infectious Diseases https://www.niaid.nih.gov/research/ted-c-pierson-phd Ted (accessed May 4, 2020).

(71) Makhluf, H.; Kim, K.; Shresta, S. Novel Strategies for Discovering Inhibitors of Dengue and Zika Fever. *Expert Opin. Drug Discov.* **2016**, *11* (10), 921–923. https://doi.org/10.1080/17460441.2016.1212013.

(72) Noble, C. G.; Chen, Y. L.; Dong, H.; Gu, F.; Lim, S. P.; Schul, W.; Wang, Q. Y.; Shi, P. Y. Strategies for Development of Dengue Virus Inhibitors. *Antiviral Res.* **2010**, *85* (3), 450–462. https://doi.org/10.1016/j.antiviral.2009.12.011.

(73) Bies, C.; Lehr, C. M.; Woodley, J. F. Lectin-Mediated Drug Targeting: History and Applications. *Adv. Drug Deliv. Rev.* **2004**, *56* (4), 425–435. https://doi.org/10.1016/j.addr.2003.10.030.

(74) Paulista, U. E.; Em, P. D. E. P.; Biológicas, C. *Dermatology in General Medicine*.

(75) Ambrosi, M.; Cameron, N. R.; Davis, B. G. Lectins: Tools for the Molecular Understanding of the Glycocode. *Org. Biomol. Chem.* **2005**, *3* (9), 1593–1608. https://doi.org/10.1039/b414350g.

(76) Hamid, R.; Masood, A.; Wani, I. H.; Rafiq, S. Lectins: Proteins with Diverse Applications. *J. Appl. Pharm. Sci.* **2013**, *3* (4SUPPL.1). https://doi.org/10.7324/JAPS.2013.34.S18.

(77) Kumar, K. K.; K., L. P. C.; J., S.; G., S. R.; P., C. S.; R., R. B. V. Biological Role of Lectins: A Review. *J. Orofac. Sci.* **2012**, *4* (1), 20–25. https://doi.org/10.4103/0975-8844.99883.

(78) Taniguchi, N.; Endo, T.; Hart, G. W.; Seeberger, P. H.; Wong, C. H. *Glycoscience: Biology and Medicine*; Taniguchi, N., Endo, T., Hart, G. W., Seeberger, P. H., Wong, C. H., Eds.; Springer Japan, 2015. https://doi.org/10.1007/978-4-431-54841-6.

(79) Yamasaki, S. *C-Type Lectin Receptors in Immunity*; Springer Japan, 2016. https://doi.org/10.1007/978-4-431-56015-9.

(80) Anderluh, M. DC-SIGN Antagonists – A Paradigm of C-Type Lectin Binding Inhibition. *Carbohydrates- Compr. Stud. Glycobiol. Glycotechnol.* **2012**, 137–160.

https://doi.org/http://dx.doi.org/10.5772/50627.

(81)   Guo, Y.; Feinberg, H.; Conroy, E.; Mitchell, D. A.; Alvarez, R.; Blixt, O.; Taylor, M. E.; Weis, W. I.; Drickamer, K. Structural Basis for Distinct Ligand-Binding and Targeting Properties of the Receptors DC-SIGN and DC-SIGNR. *Nat. Struct. Mol. Biol.* **2004**, *11* (7), 591–598. https://doi.org/10.1038/nsmb784.

(82)   Lozach, P.; Burleigh, L.; Staropoli, I.; Amara, A. The C Type Lectins DC-SIGN and L-SIGN: Receptors for Viral Glycoproteins. *Glycolvirology Protoc.* **2007**, 51–68. https://doi.org/10.1007/978-1-59745-393-6_4.

(83)   Saba, K.; Denda-Nagai, K.; Irimura, T. A C-Type Lectin MGL1/CD301a Plays an Anti-Inflammatory Role in Murine Experimental Colitis. *Am. J. Pathol.* **2009**, *174* (1), 144–152. https://doi.org/10.2353/ajpath.2009.080235.

(84)   Pharmaceuticals, A. Antibodies to the C-Type Lectin, L-SIGN, as Tentative Therapeutic Agents for Induction of Antigen-Specific Tolerance. *Expert Opin. Ther. Pat.* **2007**, *17* (2), 243–250. https://doi.org/10.1517/13543776.17.2.243.

(85)   Švajger, U.; Anderluh, M.; Jeras, M.; Obermajer, N. C-Type Lectin DC-SIGN: An Adhesion, Signalling and Antigen-Uptake Molecule That Guides Dendritic Cells in Immunity. *Cell. Signal.* **2010**, *22* (10), 1397–1405. https://doi.org/10.1016/j.cellsig.2010.03.018.

(86)   Geijtenbeek, T. B. .; Torensma, R.; van Vliet, S. J.; van Duijnhoven, G. C. .; Adema, G. J.; van Kooyk, Y.; Figdor, C. G. Identification of DC-SIGN, a Novel Dendritic Cell–Specific ICAM-3 Receptor That Supports Primary Immune Responses. *Cell* **2000**, *100* (5), 575–585. https://doi.org/10.1016/S0092-8674(00)80693-5.

(87)   Itano, M. S.; Neumann, A. K.; Liu, P.; Zhang, F.; Gratton, E.; Parak, W. J.; Thompson, N. L.; Jacobson, K. DC-SIGN and Influenza Hemagglutinin Dynamics in Plasma Membrane Microdomains Are Markedly Different. *Biophys. J.* **2011**, *100* (11), 2662–2670. https://doi.org/10.1016/j.bpj.2011.04.044.

(88)   Hao, L.; Zhou, T.; Zhang, Y.; Chen, Y. DC-SIGN and Immunoregulation. *Cell. Mol. Immunol.* **2006**, *3* (4), 279–283.

(89)   Menon, S.; Rosenberg, K.; Graham, S. A.; Ward, E. M.; Taylor, M. E.; Drickamer, K.;

Leckband, D. E. Binding-Site Geometry and Flexibility in DC-SIGN Demonstrated with Surface Force Measurements. *Proc. Natl. Acad. Sci. U. S. A.* **2009**, *106* (28), 11524–11529. https://doi.org/10.1073/pnas.0901783106.

(90)   Anderluh, M.; Jug, G.; Svajger, U.; Obermajer, N. DC-SIGN Antagonists, a Potential New Class of Anti-Infectives. *Curr. Med. Chem.* **2012**, *19* (7), 992–1007. https://doi.org/10.2174/092986712799320664.

(91)   Valladeau, J.; Ravel, O.; Dezutter-Dambuyant, C.; Moore, K.; Kleijmeer, M.; Liu, Y.; Duvert-Frances, V.; Vincent, C.; Schmitt, D.; Davoust, J.; Caux, C.; Lebecque, S.; Saeland, S. Langerin, a Novel C-Type Lectin Specific to Langerhans Cells, Is an Endocytic Receptor That Induces the Formation of Birbeck Granules. *Immunity* **2000**, *12* (1), 71–81. https://doi.org/10.1016/S1074-7613(00)80160-0.

(92)   Chabrol, E.; Nurisso, A.; Daina, A.; Vassal-Stermann, E.; Thepaut, M.; Girard, E.; Vivès, R. R.; Fieschi, F. Glycosaminoglycans Are Interactants of Langerin: Comparison with Gp120 Highlights an Unexpected Calcium-Independent Binding Mode. *PLoS One* **2012**, *7* (11), 1–12. https://doi.org/10.1371/journal.pone.0050722.

(93)   McGreal, E. P.; Martinez-Pomares, L.; Gordon, S. Divergent Roles for C-Type Lectins Expressed by Cells of the Innate Immune System. *Mol. Immunol.* **2004**, *41* (11), 1109–1121. https://doi.org/10.1016/j.molimm.2004.06.013.

(94)   Tada, Y.; Riedl, E.; Lowenthal, M. S.; Liotta, L. A.; Briner, D. M.; Crouch, E. C.; Udey, M. C. Identification and Characterization of Endogenous Langerin Ligands in Murine Extracellular Matrix. *J. Invest. Dermatol.* **2006**, *126* (7), 1549–1558. https://doi.org/10.1038/sj.jid.5700283.

(95)   Sutkeviciute, L.; Fieschi, F. Human Immunodeficiency Virus: The infection via Sexual Transmission - Structure and function of C-type lectin receptor DC-SIGN DC-SIGN https://glycopedia.eu/e-chapters/Human-Immunodeficiency-Virus-the/Structure-and-function-of-C-type%0AStructure.

(96)   Van Der Vlist, M.; Geijtenbeek, T. B. H. Langerin Functions as an Antiviral Receptor on Langerhans Cells. *Immunol. Cell Biol.* **2010**, *88* (4), 410–415. https://doi.org/10.1038/icb.2010.32.

(97)   Cecioni, S.; Imberty, A.; Vidal, S. Glycomimetics Versus Multivalent Glycoconjugates

for the Design of High Affinity Lectin Ligands. *Chem. Rev.* **2015**, *115* (1), 525–561. https://doi.org/10.1021/cr500303t.

(98) McNaught, A. D.; Wilkinson, A. Gold Book - Carbohydrates https://goldbook.iupac.org/terms/view/C00820. https://doi.org/doi.org/10.1351/goldbook.C00820.

(99) Gim, S.; Zhu, Y.; Seeberger, P. H.; Delbianco, M. Carbohydrate-Based Nanomaterials for Biomedical Applications. *Wiley Interdiscip. Rev. Nanomedicine Nanobiotechnology* **2019**, *11* (5). https://doi.org/10.1002/wnan.1558.

(100) Varki, A. Biological Roles of Glycans. *Glycobiology* **2017**, *27* (1), 3–49. https://doi.org/10.1093/glycob/cww086.

(101) Eykman, J. F. The Botanical Relations of Illicium Religiosum, Sieb., Illicium Anisatum, Lour. * | Henriette's Herbal Homepage http://www.henriettes-herb.com/eclectic/journals/ajp/ajp1881/08-illicium.html.

(102) Payne, R.; Edmonds, M. Isolation of Shikimic Acid from Star Aniseed. *J. Chem. Educ.* **2005**, *82* (4), 599–600. https://doi.org/10.1021/ed082p599.

(103) Panche, A. N.; Diwan, A. D.; Chandra, S. R. Flavonoids: An Overview. *J. Nutr. Sci.* **2016**, *5* (47), 1–15. https://doi.org/10.1017/jns.2016.41.

(104) Wang, G.-W.; Wen-Ting Hu; Huang, B.-K.; Qin, L.-P. Illicium Verum: A Review on Its Botany, Traditional Use, Chemistry and Pharmacology. *J. Ethnopharmacol.* **2011**, *136* (1), 10–20. https://doi.org/10.1016/j.jep.2011.04.051.

(105) M. Estévez, A.; J. Estévez, R. A Short Overview on the Medicinal Chemistry of (—)-Shikimic Acid. *Mini-Reviews Med. Chem.* **2012**, *12* (14), 1443–1454. https://doi.org/10.2174/138955712803832735.

(106) Ghosh, S.; Chisti, Y.; Banerjee, U. C. Production of Shikimic Acid. *Biotechnol. Adv.* **2012**, *30* (6), 1425–1431. https://doi.org/10.1016/j.biotechadv.2012.03.001.

(107) Borah, J. C. Shikimic Acid: A Highly Prospective Molecule in Pharmaceutical Industry. *Curr. Sci.* **2015**, *109* (9), 1–8. https://doi.org/10.18520/v109/i9/1672-1679.

(108) Quiroz, D. C. D.; Carmona, S. B.; Bolívar, F.; Escalante, A. Current Perspectives on Applications of Shikimic and Aminoshikimic Acids in Pharmaceutical Chemistry. *Res.*

Reports Med. Chem. **2014**, *4*, 35–46. https://doi.org/10.2147/rrmc.s46560.

(109) Garbossa, W. A. C.; Mercurio, D. G.; Campos, P. M. B. G. M. Shikimic Acid: A Potential Active Principle for Skin Exfoliation. *Surg. Cosmet. Dermatology* **2014**, *6* (3), 239–247.

(110) Rawat, G.; Tripathi, P.; Saxena, R. K. Expanding Horizons of Shikimic Acid: Recent Progresses in Production and Its Endless Frontiers in Application and Market Trends. *Appl. Microbiol. Biotechnol.* **2013**, *97* (10), 4277–4287. https://doi.org/10.1007/s00253-013-4840-y.

(111) Bochkov, D. V.; Sysolyatin, S. V.; Kalashnikov, A. I.; Surmacheva, I. A. Shikimic Acid: Review of Its Analytical, Isolation, and Purification Techniques From Plant and Microbial Sources. *J. Chem. Biol.* **2012**, *5* (1), 5–17. https://doi.org/10.1007/s12154-011-0064-8.

(112) Commision, E. Definition of a nanomaterial http://ec.europa.eu/environment/chemicals/nanotech/faq/definition_en.htm%0ADefiniti on (accessed Mar 25, 2019).

(113) Kim E. Sapsford, W. Russ Algar, Lorenzo Berti, Kelly Boeneman Gemmill, Brenda J. Casey, Eunkeu Oh, M. H. S. and I. L. M. Functionalizing Nanoparticles With Biological Molecules: Developing Chemistries That Facilitate Nanotechnology. *Chem. Rev.* **2013**, *113* (3), 1904−2074. https://doi.org/10.1021/cr300143v.

(114) Mody, V.; Siwale, R.; Singh, A.; Mody, H. Introduction to Metallic Nanoparticles. *J. Pharm. Bioallied Sci.* **2010**, *2* (4), 282–289. https://doi.org/10.4103/0975-7406.72127.

(115) Cao, G.; Wang, Y. *Nanostrutures and Nanomaterials - Synthesis, Properties, and Applications*, 2nd ed.; World Scientific Publishing Co. Pte. Ltd.: Singapore, 2013.

(116) Shi, J.; Votruba, A. R.; Farokhzad, O. C.; Langer, R. Nanotechnology in Drug Delivery and Tissue Engineering: From Discovery to Applications. *Nano Lett.* **2010**, *10* (9), 3223–3230. https://doi.org/10.1021/nl102184c.

(117) Hornyak, G. L.; Dutta, J.; Tibbbals, H. F.; Rao, A. K. *Introduction to Nanoscience*; CRC Press: New York, 2008.

(118) Egorova, E. M.; Kubatiev, A. A.; Schvets, V. I. *Biological Effects of Metal Nanoparticles*, 1st ed.; Springer, Ed.; Springer International Publishing: Switzerland, 2016.

https://doi.org/10.1007/978-3-319-30906-4.

(119) Rai, M.; Shegokar, R. *Metal Nanoparticles in Pharma*, 1st ed.; Rai, M., Shegokar, R., Eds.; Springer International Publishing, 2017. https://doi.org/10.1007/978-3-319-63790-7.

(120) Franci, G.; Falanga, A.; Galdiero, S.; Palomba, L.; Rai, M.; Morelli, G.; Galdiero, M. Silver Nanoparticles as Potential Antibacterial Agents. *Molecules* **2015**, *20* (5), 8856–8874. https://doi.org/10.3390/molecules20058856.

(121) Schlesinger, M. E.; King, M. J.; Sole, K. C.; Davenport, W. G. *Extractive Metallurgy of Copper*, 5th ed.; Elsevier, 2019.

(122) Antonijevic, M. M.; Petrovic, M. B. Copper Corrosion Inhibitors. A Review. *Int. J. Electrochem. Sci.* **2008**, *3* (1), 1–28. https://doi.org/10.1016/j.ijengsci.2004.12.001.

(123) Atkins, P.; Overton, T.; Rourke, J.; Weller, M.; Armstrong, F. *Inorganic Chemistry*, 5th ed.; W. H. FREEMAN & COMPANY: New York, 2010. https://doi.org/10.1007/978-1-84628-986-6_2.

(124) Berg, J. M.; Tymoczko, J. L.; Stryer, L. *Biochemistry*, 5th ed.; 2013.

(125) Araya, M.; Olivares, M.; Pizarro, F. Copper in Human Health. *Int. J. Environ. Heal.* **2007**, *1* (4), 608–620. https://doi.org/10.1504/IJENVH.2007.018578.

(126) Panel on Micronutrients, S. on U. R. L. of N. and of I. *Dietary Reference Intakes for Vitamin A, Vitamin K, Arsenic, Boron, Chromium, Copper, Iodine, Iron, Manganese, Molybdenum, Nickel, Silicon, Vanadium, and Zinc: A Report of the Panel on Micronutrients, ...*, 1st ed.; National Academies Press, 2002.

(127) Morrison, J. Copper's Virus-Killing Powers Were Known Even to the Ancients https://www.smithsonianmag.com/science-nature/copper-virus-kill-180974655/%250.

(128) Michels, H. T.; Keevil, C. W.; Salgado, C. D.; Schmidt, M. G. From Laboratory Research to a Clinical Trial: Copper Alloy Surfaces Kill Bacteria and Reduce Hospital-Acquired Infections. *Heal. Environ. Res. Des. J.* **2015**, *9* (1), 64–79. https://doi.org/10.1177/1937586715592650.

(129) Jain, K.; Kesharwani, P.; Gupta, U.; Jain, N. K. Dendrimer Toxicity: Let's Meet the Challenge. *Int. J. Pharm.* **2010**, *394* (1–2), 122–142.

https://doi.org/10.1016/j.ijpharm.2010.04.027.

(130) Bulhleier, E.; Wehner, W.; Vögtle, F. "Cascade"- and "Nonskid-Chain-like" Syntheses of Molecular Cavity Topologies. *Synthesis (Stuttg).* **1978**, *1978*, 155–158. https://doi.org/10.1055/s-1978-24702.

(131) Tomalia, D. A.; Baker, H.; Dewald, J.; Hall, M.; Kallos, G.; Martin, S.; Roeck, J.; Ryder, J.; Smith, P. A New Class of Polymers: Starburst-Dendritic Macromolecules. *Polym. J.* **1985**, *17* (1), 117–132. https://doi.org/10.1295/polymj.17.117.

(132) Bharali, D. J.; Khalil, M.; Gurbuz, M.; Simone, T. M.; Mousa, S. A. Nanoparticles and Cancer Therapy: A Concise Review with Emphasis on Dendrimers. *Int. J. Nanomedicine* **2009**, *4* (1), 1–7.

(133) Newkome, G. R.; Yao, Z.-Q.; Baker, G. R.; Gupta, V. K. Cascade Molecules: A New Approach to Micelles. *J. Org. Chem.* **1985**, *50* (11), 2003–2004. https://doi.org/10.1021/jo00211a052.

(134) Tomalia, D. A.; Fréchet, M. J. *Dendrimers and Other Dendritic Polymers*; Dr. John Scheirs, Ed.; Wiley: London, UK, 2001; Vol. 1.

(135) Liu, M.; Fréchet, J. M. J. Designing Dendrimers for Drug Delivery. *Pharm. Sci. Technolo. Today* **1999**, *2* (10), 393–401. https://doi.org/10.1016/S1461-5347(99)00203-5.

(136) Augustus, E. N.; Allen, E. T.; Nimibofa, A.; Donbebe, W. A Review of Synthesis, Characterization and Applications of Functionalized Dendrimers. *Am. J. Polym. Sci.* **2017**, *7* (1), 8–14. https://doi.org/10.5923/j.ajps.20170701.02.

(137) Vögtle, F.; Richardt, G.; Werner, N. *Dendrimer Chemistry - Concepts, Syntheses, Properties, Applications*; Wiley-VCH: Weinheim, 2009. https://doi.org/10.1002/9783527626953.

(138) Dufès, C.; Uchegbu, I. F.; Schätzlein, A. G. Dendrimers in Gene Delivery. *Adv. Drug Deliv. Rev.* **2005**, *57* (15), 2177–2202. https://doi.org/10.1016/j.addr.2005.09.017.

(139) Kumbar, S. G.; Laurencin, C. T.; Deng, M. *Natural and Synthetic Biomedical Polymers*; Kumbar, S. G., Laurencin, C. T., Deng, M., Eds.; Elsevier, 2014. https://doi.org/10.1016/C2011-0-07330-1.

(140) de Araújo, R. V.; da Silva Santos, S.; Ferreira, E. I.; Giarolla, J. New Advances in General Biomedical Applications of PAMAM Dendrimers. *Molecules* **2018**, *23* (11), 1–27. https://doi.org/10.3390/molecules23112849.

(141) Malkoch, M.; Malmström, E.; Nyström, A. M. Dendrimers: Properties and Applications. In *Polymer Science: A Comprehensive Reference*; Elsevier B.V., 2012; Vol. 6, pp 113–176. https://doi.org/10.1016/B978-0-444-53349-4.00162-X.

(142) Duncan, R.; Izzo, L. Dendrimer Biocompatibility and Toxicity. *Adv. Drug Deliv. Rev.* **2005**, *57* (15), 2215–2237. https://doi.org/10.1016/j.addr.2005.09.019.

(143) Gillies, E. R.; Fréchet, J. M. J. PH-Responsive Copolymer Assemblies for Controlled Release of Doxorubicin. *Bioconjug. Chem.* **2005**, *16* (2), 361–368. https://doi.org/10.1021/bc049851c.

(144) Mecke, A.; Lee, I.; Baker, J. R.; Holl, M. M. B.; Orr, B. G. Deformability of Poly(Amidoamine) Dendrimers. *Eur. Phys. J. E* **2004**, *14* (1), 7–16. https://doi.org/10.1140/epje/i2003-10087-5.

(145) Gawande, M. B.; Goswami, A.; Felpin, F. X.; Asefa, T.; Huang, X.; Silva, R.; Zou, X.; Zboril, R.; Varma, R. S. Cu and Cu-Based Nanoparticles: Synthesis and Applications in Catalysis. *Chem. Rev.* **2016**, *116* (6), 3722–3811. https://doi.org/10.1021/acs.chemrev.5b00482.

(146) Maity, P.; Yamazoe, S.; Tsukuda, T. Dendrimer-Encapsulated Copper Cluster as a Chemoselective and Regenerable Hydrogenation Catalyst. *ACS Catal.* **2013**, *3* (2), 182–185. https://doi.org/10.1021/cs3007318.

(147) Varshney, R.; Bhadauria, S.; Gaur, M. S.; Pasricha, R. Characterization of Copper Nanoparticles Synthesized by a Novel Microbiological Method. *J. Miner. Met. Mater. Soc.* **2010**, *62* (12), 102–104. https://doi.org/10.1007/s11837-010-0171-y.

(148) Feng, Z. V.; Lyon, J. L.; Croley, J. S.; Crooks, R. M.; Bout, D. A. Vanden; Stevenson, K. J. Synthesis and Catalytic Evaluation of Dendrimer-Encapsulated Cu Nanoparticles An Undergraduate Experiment Exploring Catalytic Nanomaterials. *J. Chem. Educ.* **2009**, *86* (3), 368–372. https://doi.org/10.1021/ed086p368.

(149) Zhao, M.; Sun, L.; Crooks, R. M. Preparation of Cu Nanoclusters Within Dendrimer

Templates. *J. Am. Chem. Soc.* **1998**, *120* (19), 4877–4878. https://doi.org/10.1021/ja980438n.

(150) Nemanashi, M.; Meijboom, R. Synthesis and Characterization of Cu, Ag and Au Dendrimer-Encapsulated Nanoparticles and Their Application in the Reduction of 4-Nitrophenol to 4-Aminophenol. *J. Colloid Interface Sci.* **2013**, *389* (1), 260–267. https://doi.org/10.1016/j.jcis.2012.09.012.

(151) Tang, Y. H.; Cangiotti, M.; Kao, C. L.; Ottaviani, M. F. EPR Characterization of Copper(II) Complexes of PAMAM-Py Dendrimers for Biocatalysis in the Absence and Presence of Reducing Agents and a Spin Trap. *J. Phys. Chem. B* **2017**, *121* (46), 10498–10507. https://doi.org/10.1021/acs.jpcb.7b09464.

(152) Zhao, M.; Crooks, R. M. Intradendrimer Exchange of Metal Nanoparticles. *Chem. Mater.* **1999**, *11* (11), 3379–3385. https://doi.org/10.1021/cm990435p.

(153) Liu, Q.-M.; Yasunami, T.; Kuruda, K.; Okido, M. Preparation of Cu Nanoparticles with Ascorbic Acid by Aqueous Solution Reduction Method. *Trans. Nonferrous Met. Soc. China* **2012**, *22* (9), 2198–2203. https://doi.org/10.1016/S1003-6326(11)61449-0.

(154) Pavia, D. L.; Lampman, G. M.; Kriz, G. S. *Introduction to Spectroscopy, A Guide For Students of Organic Chemistry*, 3rd ed.; Brooks Cole: USA, 2000.

(155) Lu, Y. Z.; Wei, W. T.; Chen, W. Copper Nanoclusters: Synthesis, Characterization and Properties. *Chinese Sci. Bull.* **2012**, *57* (1), 41–47. https://doi.org/10.1007/s11434-011-4896-y.

(156) Blümich, B. Introduction to Compact NMR: A Review of Methods. *TrAC - Trends Anal. Chem.* **2016**, *83* (Part A), 2–11. https://doi.org/10.1016/j.trac.2015.12.012.

(157) Gundlach, M.; Paulsen, K.; Garry, M.; Lowry, S. Yin and Yang in Chemistry Education: The Complementary Nature of FT-IR and NMR Spectroscopies. *Thermo Fish. Sci.* **2015**, 1–6.

(158) Bhattacharjee, S. DLS and Zeta Potential - What They Are and What They Are Not? *J. Control. Release* **2016**, *235*, 337–351. https://doi.org/10.1016/j.jconrel.2016.06.017.

(159) Johari, O.; Bhattacharyya, S. The Application of Scanning Electron Microscopy for the Characterization of Powders. *Powder Technol.* **1969**, *2* (6), 335–348.

https://doi.org/10.1016/0032-5910(69)80026-4.

(160) Gawande, M. B.; Goswami, A.; Felpin, F. X.; Asefa, T.; Huang, X.; Silva, R.; Zou, X.; Zboril, R.; Varma, R. S. Cu and Cu-Based Nanoparticles: Synthesis and Applications in Catalysis. *Chem. Rev.* **2016**, *116* (6), 3722–3811. https://doi.org/10.1021/acs.chemrev.5b00482.

(161) Leonard, D. N.; Chandler, G. W.; Seraphin, S. Scanning Electron Microscopy. In *Characterization of Materials*; Kaufmann, E. N., Ed.; John Wiley & Sons, Inc.: Hoboken, NJ, USA, 2012; pp 1721–1736. https://doi.org/10.1002/0471266965.com081.pub2.

(162) Boss, C. B.; Fredeen, K. J. *Concepts, Instrumentation and Techniques in Coupled Plasma Optical Emission Spectrometry*, 3rd ed.; PerkinElmer Life and Analytical Sciences: Shelton, 2004.

(163) Ngomuo, A. J.; Jones, R. S. Cytotoxicity Studies of Quercetin, Shikimate, Cyclohexanecarboxylate and Ptaquiloside (FALTA O DOI). *Vet. Hum. Toxicol.* **1996**, *38* (1), 14–18.

(164) Zeng, Y.; Kurokawa, Y.; Win-Shwe, T.-T.; Zeng, Q.; Hirano, S.; Zhang, Z.; Sone, H. Effects of PAMAM Dendrimers With Various Surface Functional Groups and Multiple Generations on Cytotoxicity and Neuronal Differentiation Using Human Neural Progenitor Cells. *J. Toxicol. Sci.* **2016**, *41* (3), 351–370. https://doi.org/10.2131/jts.41.351.

(165) Riss, T. L.; Moravec, R. A.; Niles, A. L.; Duellman, S.; Benink, H. A.; Worzella, T. J.; Minor, L. Cell Viability Assays. In *Assay Guidance Manual [Internet]*; 2013; Vol. 114, pp 785–796. https://doi.org/10.1016/j.acthis.2012.01.006.

(166) Crooks, R. M.; Zhao, M.; Sun, L.; Chechik, V.; Yeung, L. K. Dendrimer-Encapsulated Metal Nanoparticles: Synthesis, Characterization, and Applications to Catalysis. *Acc. Chem. Res.* **2001**, *34* (3), 181–190. https://doi.org/10.1021/ar000110a.

(167) Matallo, M. B.; Almeida, S. D. B.; Cerdeira, A. L.; Franco, D. A.; Blanco, F. M. G.; Menezes, P. T. C.; Luchini, L. C.; Moura, M. A. M.; Duke, S. O. Microwave-Assisted Solvent Extraction and Analysis of Shikimic Acid from Plant Tissues. *Planta Daninha* **2009**, *27* (SPECIAL ISSUE.), 987–994. https://doi.org/10.1590/s0100-83582009000500012.

(168) Scannell, J. P.; Helen, A. A.; Morris, W. Modern Approach to the Isolation and Characterization of L-Ascorbic Acid (Vitamin C). *J. Agric. Food Chem.* **1974**, *22* (3), 538–539. https://doi.org/10.1021/jf60193a010.

(169) Berger, S.; Sicker, D. *Classics in Spectroscopy - Isolation and Structure Elucidation of Natural Products*; Wiley-VCH, 2009.

(170) Pande, S. &; Crooks, R. M. Analysis of Poly(Amidoamine) Dendrimer Structure by UV-Vis Spectroscopy. *Langmuir* **2011**, *27* (15), 9609–9613. https://doi.org/10.1021/la201882t.

(171) Crooks, R. M.; Lemon III, B. I.; Sun, L.; Yeung, L. K.; Zhao, M. Dendrimer-Encapsulated Metals and Semiconductors: Synthesis, Characterization and Applications. In *Topics in Current Chemistry*; Vögtle, F., Ed.; Springer: Berlin, 2001; Vol. 212, pp 81–135. https://doi.org/https://doi.org/10.1007/3-540-44924-8_3.

(172) Wang, D.; Imae, T. Fluorescence Emission from Dendrimers and Its PH Dependence. *J. Am. Chem. Soc.* **2004**, *126* (41), 13204–13205. https://doi.org/10.1021/ja0454992.

(173) Wada, H.; Kido, T.; Tanaka, N.; Murakami, T.; Saiki, Y.; Chen, C.-M. Chemical and Chemotaxonomical Studies of Ferns. LXXXI. Characteristic Lignans of Blechnaceous Ferns. *Chem. Pharm. Bull.* **1992**, *40* (8), 2099–2101. https://doi.org/10.1248/cpb.40.2099.

(174) Yohannan Panicker, C.; Tresa Varghese, H.; Philip, D. FT-IR, FT-Raman and SERS Spectra of Vitamin C. *Spectrochim. Acta - Part A Mol. Biomol. Spectrosc.* **2006**, *65* (3–4), 802–804. https://doi.org/10.1016/j.saa.2005.12.044.

(175) Gautam, S. P.; Gupta, A. K.; Sharma, A.; Gautam, T.; Kaundal, M. Synthesis and Analytical Characterization of Ester and Amine Terminated PAMAM Dendrimers. *Glob. J. Med. Res. Pharma, Drug Discov. Toxicol. Med.* **2013**, *13* (3), 1–9.

(176) Reid, R. S. The Proton NMR Spectrum of Ascorbic Acid: A Relevant Example of Deceptively Simple Second-Order Behavior. *J. Chem. Educ.* **1989**, *66* (4), 344–345. https://doi.org/10.1021/ed066p344.

(177) Hung, W.-I.; Hung, C.-B.; Chang, Y.-H.; Dai, J.-K.; Li, Y.; He, H.; Chen, S.-W.; Huang, T.-C.; Wei, Y.; Jia, X.-R.; Yeh, J.-M. Synthesis and Electroactive Properties of

Poly(Amidoamine) Dendrimers With an Aniline Pentamer Shell. *J. Mater. Chem.* **2011**, *21* (12), 4581–4587. https://doi.org/10.1039/c0jm03876h.

(178) Nishikawa, Y.; Kurata, T. Interconversion Between Dehydro-L-Ascorbic Acid and L-Ascorbic Acid. *Biosci. Biotechnol. Biochem.* **2000**, *64* (3), 476–483. https://doi.org/10.1271/bbb.64.476.

(179) Nemet, I.; Monnier, V. M. Vitamin C Degradation Products and Pathways in the Human Lens. *J. Biol. Chem.* **2011**, *286* (43), 37128–37136. https://doi.org/10.1074/jbc.M111.245100.

(180) Jevprasesphant, R.; Penny, J.; Jalal, R.; Attwood, D.; McKeown, N. B.; D'Emanuele, A. The Influence of Surface Modification on the Cytotoxicity of PAMAM Dendrimers. *Int. J. Pharm.* **2003**, *252* (1–2), 263–266. https://doi.org/10.1016/S0378-5173(02)00623-3.

7.   ANNEX

7.1.   Characterization

7.1.1.   NMR

Table 5 – ^{1}H NMR signals, corresponding multiplicity, area and signal attribution to the shikimic acid structure.

δ (ppm)	Multiplicity	Area	Proton amount	Proton type
2.201 – 2.263	dd	1.026	1	a
2.718 – 2.776	dd	1.026	1	b
3.768 – 3.799	q	1.022	1	c
4.019 – 4.069	q	1.026	1	d
4.460	s	1.030	1	e
6.831 – 6.840	t	1.000	1	f

Table 6 – ^{1}H NMR signals, corresponding multiplicity, area and signal attribution to the ascorbic acid structure.

δ (ppm)	Multiplicity	Area	Proton amount	Proton type
3.712 – 3.789	d	1.000	2	g
4.051 – 4.088	t	0.494	1	h
4.959 – 4.964	d	0.499	1	i

Table 7 – ^{1}H NMR signals, corresponding multiplicity, area and signal attribution to the G4 (right) and G5 (left) PAMAM dendrimer's structures.

δ (ppm)		Multiplicity		Area		Proton amount		Group	
G4	G5	G4	G5	G4	G5	G4	G5	G4	G5
2.409 – 2.443	2.408 – 2.441	t		1.000	1.000	251	498	k	
2.603 – 2.635	2.616 – 2.632	t		0.520	0.530	131	263	j	
2.759 – 2.832	2.769 – 2.829	q (should be a triplet because it is next to a CH$_2$ group)*		1.438	1.484	361	738	l	
3.221 – 3.287	3.219 – 3.284	m		1.010	1.047	254	520	m	

although the spectrum clearly presents a signal with a certain multiplicity, the data handling software interpreted the signal as having another, this can be overcome by increasing the number of scans used to obtain the sample's spectrum.

Table 8 – ^{1}H NMR signals, corresponding multiplicity, area and signal attribution to the SAG4 (right) and SAG5 (left) PAMAM dendrimer's structures.

δ (ppm)		Multiplicity		Area		Proton amount		Group	
SAG4	SAG5	SAG4	SAG5	SAG4	SAG5	SAG4	SAG5	SAG4	SAG5
2.167 – 2.221	2.164 – 2.265	t		1.000	1.000	31	59	a	
2.395 – 2.525	2.369 – 2.489	d		8.104	8.217	247	485	k	
2.686 – 2.776	2.639 – 2.776	q		4.952	4.459	151	263	j	
2.924	2.955							l	
3.130 – 3.160	3.131 – 3.160	t		6.604	5.980	201	353	b	
3.226 – 3.518	3.215 – 3.518	m		1.612	1.265	49	75	m	
3.571 – 3.742	3.667 – 3.747	s		10.791	10.472	329	619	c	
3.943 – 4.050	3.960 – 4.048	m		1.094	0.958	33	57	d	
4.371 – 4.415	4.368 – 4.412	m		1.186	1.137	36	67	e	
6.401 – 6.436	6.403	s		0.987	0.907	30	54	f	
Average number of SA functionalised (last four peaks)						*33*	*58*	-------	

Table 9 – ^{1}H NMR signals, corresponding multiplicity, area and signal attribution to the CuSAGx imp compounds.

δ (ppm)		Multiplicity		Area		Proton amount		Proton type	
CuSAG4 imp	CuSAG5 imp	CuSAG4 imp	CuSAG5 imp	CuSAG4 imp	CuSAG5 imp	CuSAG4 imp	CuSAG5 imp	CuSAG4 imp	CuSAG5 imp
3.69 – 3.78	3.69 – 3.78	d		1.00	1.00	2		g	
4.00 – 4.03	3.99 – 4.03	q		0.50	0.50	1		h	
4.51	4.51	d		0.49	0.49	1		i	

UNIVERSIDADE da MADEIRA

CQM CENTRO DE QUÍMICA DA MADEIRA

FCT Fundação para a Ciência e a Tecnologia
MINISTÉRIO DA CIÊNCIA, TECNOLOGIA E ENSINO SUPERIOR

PEst-OE/QUI/UI0674/2013

arditi agência regional para o desenvolvimento da investigação tecnologia e inovação

M1420-01-0145-FEDER-000005

Centro de Química da Madeira – CQM+ (Madeira 14-20)

Molecular Materials®
RESEARCH GROUP
MADEIRA ISLAND - PORTUGAL

Colégio dos Jesuítas
Rua dos Ferreiros - 9000-082, Funchal

Tel: +351 291 209400
Fax: +351 291 209410
Email: gabinetedareitoria@uma.pt

A Nossa
Universidade